Stereoselectivity in Chiral Fe^{III} and Ga^{III} Tris(catecholate) Complexes Effected by Nonbonded, Weakly Polar Interactions

Timothy B. Karpishin, T. D. P. Stack, and Kenneth N. Raymond*

Contribution from the Department of Chemistry, University of California, Berkeley, California 94720

Received October 30, 1992

Abstract: A series of Fe^{III} and Ga^{III} tris(catecholate) complexes of chiral terephthalamide and catecholamide ligands has been investigated in aqueous solution with respect to their stereoselective formation of the Δ or Λ coordination isomers. Stereoselectivity is effected by nonbonded, weakly polar interactions between the aryl and methyl substituents of the chiral moieties peripheral to the metal center. The diastereomeric distributions (Δ:Λ) in the complexes were studied in solution using circular dichroism (CD) spectroscopy and ^1H NMR spectroscopy. With the symmetric bidentate ligand *N,N'*-bis((*S*)-α-methylbenzyl)-2,3-dihydroxyterephthalamide (*S*-**1**), the Fe^{III} and Ga^{III} complexes, *S*-$\mathbf{1}_{Fe}$ and *S*-$\mathbf{1}_{Ga}$, exist purely in a Λ conformation in aqueous solution. The isomorphic crystal structures of Λ-*S*-$\mathbf{1}_{Fe}$ and Λ-*S*-$\mathbf{1}_{Ga}$ allow the weakly polar interactions responsible for the stereoselectivity to be identified. In addition, aryl/cation interactions between the tetramethylammonium cations and phenyl rings in the complex anions are observed in the crystal structures of Λ-*S*-$\mathbf{1}_{Fe}(Me_4N_3)$ and Λ-*S*-$\mathbf{1}_{Ga}(Me_4N)_3$. The relevance of the aryl/cation interactions to the biological binding of acetylcholine is discussed. Crystal data for *S*-$\mathbf{1}_{Fe}(Me_4N)_3 \cdot 3MeOH$: space group *I*23, a = 27.330(8) Å, V = 20414(13) Å^3, Z = 8, R (R_w) = 0.075 (0.077). Crystal data for *S*-$\mathbf{1}_{Ga}(Me_4N)_3 \cdot 3MeOH$: space group *I*23, a = 27.259(6) Å, V = 20255(12) Å^3, Z = 8, R (R_w) = 0.078 (0.076).

Introduction

Nonbonded electrostatic interactions involving aromatic groups are emerging as significant determinants of tertiary protein structure. Analyses of protein structural data have indicated that these interactions play a substantial role in the internal arrangement of aromatic residues.[1] The root of these electrostatic interactions in most cases is the high electron density of the aromatic π cloud and the subsequent interaction of the δ^- ring with the δ^+ charge of a hydrogen atom or a positively charged nitrogen atom. These interactions have been coined "weakly polar" by Burley and Petsko since they are essentially electrostatic in nature, however, they involve one or more residues that are traditionally considered nonpolar.[2]

The concept of the aromatic ring as δ^+ charge acceptor has received additional attention outside of the realm of protein stabilization. Recent studies,[3] including the crystal structure of acetylcholinesterase,[4] suggest that interactions of the positively charged tetraalkylammonium moiety of acetylcholine with the π systems of aromatic rings are crucial for recognition of the neurotransmitter at its binding sites. In addition, the hydrogen atoms of water have been shown to interact with the aromatic moieties of a calixarene[5] and very recently with benzene itself, resulting in a water–benzene hydrogen bond.[6]

We have decided to utilize weakly polar interactions to effect stereoselectivity[7] in tris-chelate Fe^{III} and Ga^{III} complexes and to investigate the stereoselectivity with systematic escalation of these nonbonded interactions. Our focus on these metal ions and the chirality of the metal–ligand complexes is a result of our interest in siderophores: iron sequestering agents secreted by bacteria.[8]

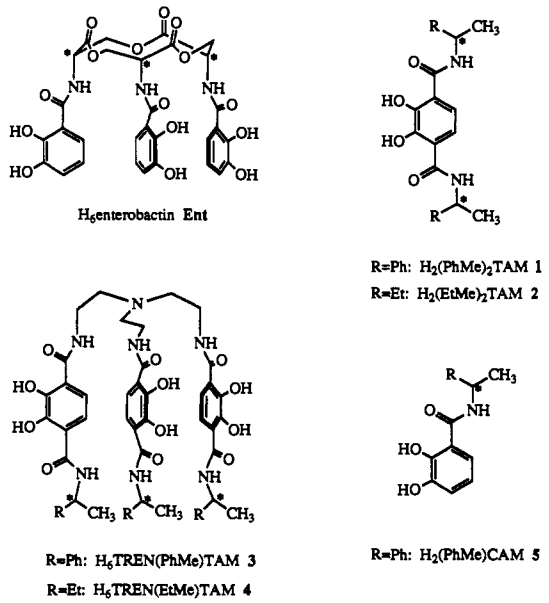

Figure 1. Chiral ligands used in this study.

More specifically, enterobactin, **Ent** (Figure 1), a siderophore produced by *Escherichia coli*, has attracted our attention due to its remarkable metal binding properties: **Ent** has the largest stability constant known for Fe^{III} ($K_f = 10^{49}$)[9] and binds labile metal ions preferentially in a Δ conformation in aqueous solution. The chirality at the metal center in $[Fe(enterobactin)]^{3-}$, $\mathbf{Ent}_{Fe}$,[10] induced by the tri-*l*-serine (*S*-chirality) lactone backbone,[11] has

* Author to whom correspondence should be addressed.

(1) Burley, S. K.; Petsko, G. A. *Science* **1985**, *229*, 23.
(2) Burley, S. K.; Petsko, G. A. *Adv. Protein Chem.* **1988**, *39*, 125.
(3) Dougherty, D. A.; Stauffer, D. A. *Science* **1990**, *250*, 1558.
(4) Sussman, J. L.; Harel, M.; Frolow, F.; Oefner, C.; Goldman, A.; Toker, L.; Silman, I. *Science* **1991**, *253*, 872.
(5) Atwood, J. L.; Hamada, F.; Robinson, K. D.; Orr, G. W.; Vincent, R. L. *Nature* **1991**, *349*, 683.
(6) Suzuki, S.; Green, P. G.; Bumgarner, R. E.; Dasgupta, S.; Goddard, W. A., III; Blake, G. A. *Science* **1992**, *257*, 942.
(7) We use the term stereoselective to indicate a preference between molecular diastereomers as defined in the following: Dunlop, J. H.; Gillard, R. D. *Adv. Inorg. Chem. Radiochem.* **1966**, *9*, 185.
(8) Matzanke, B. F.; Müller-Matzanke, G.; Raymond, K. N. In *Iron Carriers and Iron Proteins*; Loehr, T. M., Ed.; Physical Bioinorganic Chemistry Series; VCH Publishers: New York, 1989; p 1.
(9) Loomis, L. D.; Raymond, K. N. *Inorg. Chem.* **1991**, *30*, 906.
(10) Labeling scheme: The bold names or numbers refer to the ligand of a complex with the subscript indicating the appropriate metal.
(11) The crystal structure of the vanadium(IV) complex of enterobactin has recently been determined and the role of the backbone in the stereoselective formation of the Δ isomer is discussed: (a) Karpishin, T. B.; Raymond, K. N. *Angew. Chem., Int. Ed. Engl.* **1992**, *31*, 466. (b) Karpishin, T. B.; Dewey, T. M.; Raymond, K. N. *J. Am. Chem. Soc.* **1993**, *115*, 1842.

0002-7863/93/1515-6115$04.00/0

Scheme I

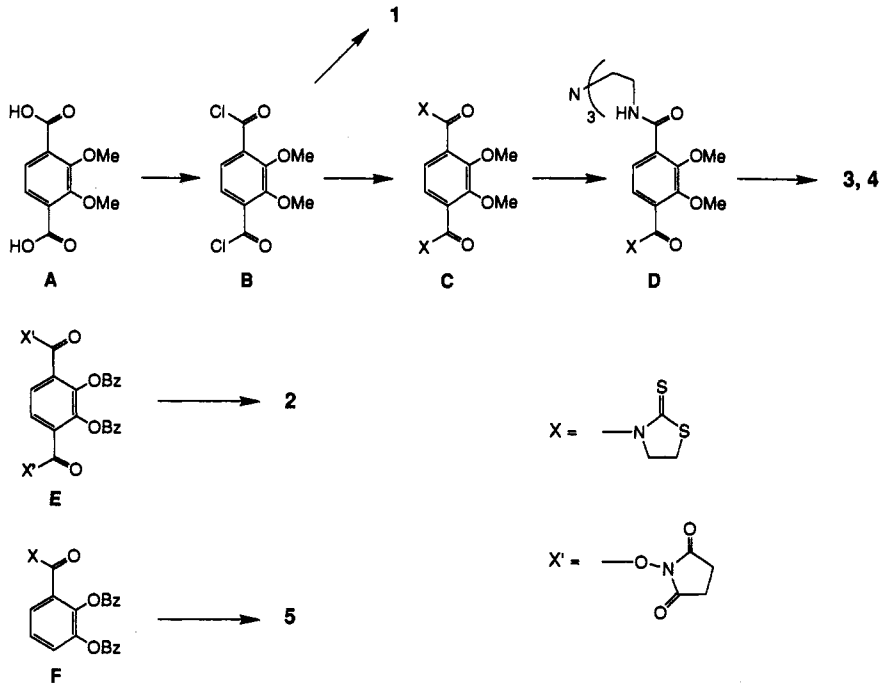

Table I. Summary of Crystallographic Data and Parameters for S-$\mathbf{1}_{Fe}(Me_4N)_3 \cdot 3MeOH$ and S-$\mathbf{1}_{Ga}(Me_4N)_3 \cdot 3MeOH$

formula	$FeC_{87}H_{114}O_{15}N_9$	$GaC_{87}H_{114}O_{15}N_9$
fw	1581.78	1595.65
temp (K)	181	173
space group	$I23$ (#197)	$I23$ (#197)
cell constants[a]		
a (Å)	27.330(8)	27.259(6)
Z	8	8
abs coeff, μ_{calc} (cm^{-1})	2.01	3.24
δ_{obs}[b] (δ_{calc}) (g cm^{-3})	1.170 (1.029)	1.168 (1.050)
V (Å^3)	20414(13)	20255(12)
crystal size (mm)	0.44 × 0.37 × 0.50	0.55 × 0.55 × 0.35
radiation	Mo Kα (λ = 0.71073 Å)	Mo Kα (λ = 0.71073 Å)
reflections measured (exclusions)	$+h, +k, +l$; ($h + k + l = 2n + 1$) and ($h > l$ or $k > l$)	$+h, +k, +l$; ($h + k + l = 2n + 1$) and ($h > l$ or $k > l$)
2θ range	$2° \le 2\theta \le 50°$	$2° \le 2\theta \le 50°$
scan type	θ–2θ	θ–2θ
scan width	0.70 + 0.35(tan θ)	0.70 + 0.35(tan θ)
scan speed (θ, deg/min)	3.3	3.3
reflections collected	3319	3299
unique reflections	3199	3180
reflections ($F_o^2 > 2.5^*\sigma(F_o^2)$)	1790	1720
no. of variables	329	327
parameter-to-variable ratio	5.4	5.3
R (R_w) (%)	7.5 (7.7)	7.8 (7.6)
final fourier ρ_{max}; ρ_{min} (e^-/Å^3)	+0.208; –0.075[c]	+0.256; –0.032[c]
largest correlation coeff	0.452	0.544

[a] In this and subsequent tables, the esd's of all parameters are given in parentheses. [b] Determined by the neutral buoyancy in CCl_4/cyclohexane. [c] Maximum positive and negative difference peaks.

been assigned by comparisons of circular dichroism (CD) spectra of resolved, kinetically inert Cr^{III} and Rh^{III} tris(catecholate) complexes with those of $\mathbf{Ent}_{Cr}$ and $\mathbf{Ent}_{Rh}$.[12] The assignment has therefore relied on the similarities in the structure of Fe^{III}, Cr^{III}, and Rh^{III} complexes since *correlated* structural and spectroscopic data of resolved Fe^{III} tris(catecholate) complexes are lacking. Absolute assignment of the tris-chelate chirality in $\mathbf{Ent}_{Fe}$ has biological relevance since the mirror image Fe^{III} enantioenterobactin complex does not support microbial growth.[13]

Two approaches to designing chiral ligands for which the Δ and Λ coordination isomers are diastereomeric, and therefore energetically nonequivalent, have been reported previously. The use of tripodal ligands which tether three chiral bidentate units represents one approach; the chiral preference at the metal center results from interactions between the linkages of the backbone which develop upon metal complexation. Synthetic analogs of **Ent** with amino acids incorporated into the ligands have been synthesized using this approach by Tor et al.[14] and by Hisaeda et al.[15] In both studies, the Fe^{III} complexes exhibit a chiral preference at the metal center as determined by CD spectroscopy; however, the absence of single crystal structural data precludes the identification of the important interactions that give rise to the chiral preferences. In addition, no attempts to determine the thermodynamic distributions of the diastereomers in solution have

(12) (a) Isied, S. S.; Kuo, G.; Raymond, K. N. *J. Am. Chem. Soc.* **1976**, *98*, 1763. (b) McArdle, J. V.; Sofen, S. R.; Cooper, S. R.; Raymond, K. N. *Inorg. Chem.* **1978**, *17*, 3075.

(13) Neilands, J. B.; Erickson, T. J.; Rastetter, W. H. *J. Biol. Chem.* **1981**, *256*, 3831.

(14) (a) Tor, Y.; Libman, J.; Shanzer, A.; Felder, C. E.; Lifson, S. *J. Am. Chem. Soc.* **1992**, *114*, 6661. (b) Tor, Y.; Libman, J.; Shanzer, A.; Lifson, S. *J. Am. Chem. Soc.* **1987**, *109*, 6517.

(15) Hisaeda, Y.; Ihara, T.; Ohno, T.; Murakami, Y. *Chem. Lett.* **1991**, 2139.

Table II. Positional Parameters for S-$\mathbf{1}_{Fe}(Me_4N)_3$·3MeOH

atom	x	y	z	B(iso)[a]	atom	x	y	z	B(iso)[a]
Fe	0.19238(5)	x	x	2.14(1)	C8A	0.1457(4)	0.3465(4)	0.4048(4)	4.4(3)
O1A	0.1874(2)	0.1976(2)	0.2660(2)	2.3(1)	C8B	0.2051(5)	-0.0558(4)	0.1190(4)	4.4(3)
O1B	0.1724(2)	0.1240(2)	0.2088(2)	2.6(2)	C9A	0.1163(4)	0.3865(5)	0.3914(4)	5.0(3)
O2A	0.1889(3)	0.1822(3)	0.4190(2)	4.6(2)	C9B	0.2444(5)	-0.0598(4)	0.0896(5)	5.3(3)
O2B	0.1562(3)	-0.0174(2)	0.2640(3)	4.4(2)	C10A	0.1102(4)	0.3985(4)	0.3445(5)	4.4(3)
N1A	0.1931(3)	0.2346(3)	0.3543(3)	3.3(2)	C10B	0.2669(5)	-0.0200(4)	0.0711(4)	5.3(3)
N1B	0.1454(3)	0.0317(3)	0.1980(3)	3.5(2)	C11A	0.1315(4)	0.3724(4)	0.3066(5)	4.7(3)
C1A	0.1790(3)	0.1558(3)	0.2879(3)	2.0(2)	C11B	0.2492(5)	0.0253(4)	0.0805(4)	5.8(4)
C1B	0.1693(3)	0.1140(4)	0.2561(3)	2.2(2)	C12A	0.1621(4)	0.3335(4)	0.3206(4)	3.9(3)
C2A	0.1784(3)	0.1497(4)	0.3393(3)	2.2(2)	C12B	0.2081(5)	0.0288(4)	0.1094(5)	5.9(4)
C2B	0.1602(4)	0.0686(3)	0.2765(4)	2.4(2)	$N(Me)_4$				
C3A	0.1684(4)	0.1021(4)	0.3574(4)	3.6(3)	N1	0.0283(3)	0.2411(4)	0.3079(4)	4.5(2)
C3B	0.1596(4)	0.0622(4)	0.3273(4)	3.3(3)	C1	-0.0149(4)	0.2139(5)	0.2900(6)	6.6(4)
C4A	0.1873(4)	0.1903(4)	0.3740(3)	2.9(2)	C2	0.0731(5)	0.2155(5)	0.2950(7)	8.8(5)
C4B	0.1526(4)	0.0238(4)	0.2466(4)	2.9(3)	C3	0.0281(5)	0.2888(5)	0.2832(6)	7.3(4)
C5A	0.2037(4)	0.2783(4)	0.3817(3)	2.7(2)	C4	0.0233(6)	0.2485(7)	0.3604(6)	9.6(6)
C5B	0.1399(5)	-0.0053(4)	0.1612(4)	4.2(3)	MeOH				
C6A	0.2562(4)	0.2915(4)	0.3747(4)	4.1(3)	O1[b]	0.4748(7)	0.0743(7)	0.1815(8)	11.7(6)*
C6B	0.0938(5)	0.0033(5)	0.1314(4)	5.4(3)	C5[b]	0.435(1)	0.050(1)	0.1503(9)	8.2(7)*
C7A	0.1701(3)	0.3200(4)	0.3682(4)	2.8(2)	O1D[b]	0.4847(9)	0.0787(8)	0.2307(9)	7.9(7)*
C7B	0.1853(4)	-0.0112(4)	0.1297(4)	3.6(3)	C5D[b]	0.484(1)	0.044(1)	0.274(1)	8(1)*

[a] The thermal parameter given for anisotropically refined atoms is the isotropic equivalent thermal parameter defined as $(4/3)[a^2B_{11} + b^2B_{22} + c^2B_{33} + ab(\cos\gamma)B_{12} + ac(\cos\beta)B_{13} + bc(\cos\alpha)B_{13}]$ where a, b, and c are real cell parameters, and B_{ij} are anisotropic β values. The starred values were refined isotropically. [b] The solvate was modeled at a 60/40 occupancy with O1 and C5 corresponding to the 60 occupancy.

Table III. Positional Parameters for S-$\mathbf{1}_{Ga}(Me_4N)_3$·3MeOH

atom	x	y	z	B(iso)[a]	atom	x	y	z	B(iso)[a]
Ga	0.19550(1)	x	x	2.332(9)	C7B	0.1900(5)	-0.0077(4)	0.1296(4)	4.7(3)
O1A	0.1913(3)	0.2010(2)	0.2683(2)	2.5(1)	C8A	0.1453(5)	0.3506(5)	0.4041(4)	4.3(3)
O1B	0.1781(2)	0.1280(2)	0.2102(2)	2.8(2)	C8B	0.2067(6)	-0.0531(4)	0.1165(5)	5.1(4)
O2A	0.1819(3)	0.1882(3)	0.4209(3)	5.6(2)	C9A	0.1105(5)	0.3856(5)	0.3921(5)	5.4(4)
O2B	0.1540(3)	-0.0138(3)	0.2648(3)	5.2(2)	C9B	0.2476(6)	-0.0570(5)	0.0848(5)	6.0(4)
N1A	0.1966(4)	0.2381(3)	0.3561(3)	3.5(2)	C10A	0.1001(5)	0.3943(5)	0.3451(6)	6.6(4)
N1B	0.1501(3)	0.0351(3)	0.1995(4)	4.0(2)	C10B	0.2707(6)	-0.0163(5)	0.0660(6)	7.7(5)
C1A	0.1819(3)	0.1595(3)	0.2895(4)	1.9(2)	C11A	0.1224(5)	0.3662(5)	0.3084(5)	5.5(3)
C1B	0.1743(4)	0.1179(4)	0.2570(4)	2.8(3)	C11B	0.2527(7)	0.0286(5)	0.0826(6)	7.9(5)
C2A	0.1792(4)	0.1529(4)	0.3417(4)	3.0(3)	C12A	0.1574(5)	0.3306(4)	0.3207(4)	4.0(3)
C2B	0.1627(4)	0.0718(4)	0.2769(4)	3.0(3)	C12B	0.2147(5)	0.0340(5)	0.1127(5)	5.6(4)
C3A	0.1675(4)	0.1074(4)	0.3591(4)	3.4(3)	$N(Me)_4$				
C3B	0.1594(4)	0.0686(4)	0.3298(4)	3.7(3)	N1	0.0277(4)	0.2329(5)	0.3204(5)	7.3(4)
C4A	0.1863(4)	0.1945(4)	0.3757(4)	3.3(3)	C1	0.0716(6)	0.2069(7)	0.317(1)	18.4(9)
C4B	0.1554(4)	0.0283(4)	0.2471(4)	3.1(3)	C2	0.0300(7)	0.2668(9)	0.2753(6)	14.1(8)
C5A	0.2039(4)	0.2834(4)	0.3834(4)	3.2(3)	C3	0.0262(7)	0.2674(7)	0.3631(6)	10.9(6)
C5B	0.1445(5)	-0.0027(5)	0.1621(4)	4.7(3)	C4	-0.0192(6)	0.2081(6)	0.315(1)	21(1)
C6A	0.2558(4)	0.2985(5)	0.3764(4)	4.2(3)	MeOH				
C6B	0.0975(5)	0.0037(6)	0.1346(5)	7.2(4)	O5	0.2966(7)	0.9677(6)	0.4043(6)	17.7(6)*
C7A	0.1686(4)	0.3215(4)	0.3685(4)	2.6(3)	C5	0.2466(8)	0.9892(9)	0.4074(8)	14.9(8)

[a] The thermal parameter given for anisotropically refined atoms is the isotropic equivalent thermal parameter defined as $(4/3)[a^2B_{11} + b^2B_{22} + c^2B_{33} + ab(\cos\gamma)B_{12} + ac(\cos\beta)B_{13} + bc(\cos\alpha)B_{13}]$ where a, b, and c are real cell parameters, and B_{ij} are anisotropic β values. The starred values were refined isotropically.

been reported. A second approach exploits nonbonded interactions between peripheral chiral appendages on bidentate chelate units. The induction of chirality at the metal center is dependent on favorable nonbonded interactions. This area has been reviewed by Ōkawa[16] whose work has shown that nonbonded interactions between chiral moieties appended to 1,3 diketone ligands in tris-chelate complexes result in stereoselectivity with labile metal ions in nonaqueous solution.[17] These studies have used ^{1}H NMR to determine the thermodynamic distributions of the isomers in solution; however, no structural analysis has been presented which identifies the interactions responsible for the stereoselectivity.

This article describes an investigation of a series of Fe^{III} and Ga^{III} complexes of chiral terephthalamide (TAM) and catecholamide (CAM) ligands (Figure 1) in which the chiral nonbonded interactions are systematically varied by changing the nature and/or the number of chiral appendages. The combination of solid state structural data with aqueous diastereomeric distributions allows the stabilizing weakly polar interactions to be identified and investigated. In addition, the use of tetraalkylammonium cations in these complexes allows a further investigation of weakly polar interactions arising between the aromatic groups of the complex anion and the ammonium cations, similar to the recognition motif suggested for acetylcholine.[3,4] Although the R_4N^+–aromatic interactions play no role in the stereoselectivity of the metal complexes, we provide evidence for the existence of the interactions in solution as well as in the solid state.[18]

Results

Ligand Syntheses. The syntheses of the ligands used in this study are depicted in Scheme I. The ligands **1**, **2**, and **5** are synthesized using either methyl or benzyl protecting groups on the catecholate oxygens and one of three activated groups for amide coupling: acyl chloride, *N*-hydroxysuccinimide ester, or 2-mercaptothiazolide. The reaction of the monocapped product **D** with 3 equiv of each chiral amine, followed by deprotection (BBr_3), provides the ligands **3** and **4** as their HBr salts.

(16) Ōkawa, H. *Coord. Chem. Rev.* **1988**, *92*, 1.
(17) Ōkawa, H.; Tokunaga, H.; Katsuki, T.; Koikawa, M.; Kida, S. *Inorg. Chem.* **1988**, *27*, 4373.

(18) A portion of these results has been previously communicated: Stack, T. D. P.; Karpishin, T. B.; Raymond, K. N. *J. Am. Chem. Soc.* **1992**, *114*, 1512.

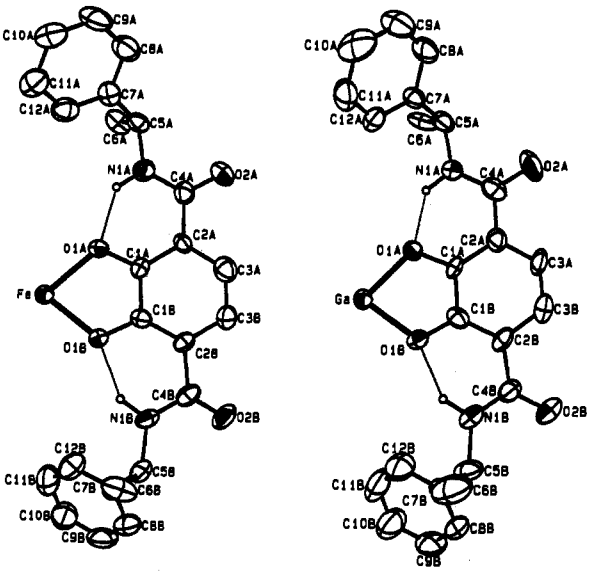

Figure 2. ORTEP drawings of one-third of the anion of S-$\mathbf{1}_{Fe}$ and S-$\mathbf{1}_{Ga}$ with the atomic thermal ellipsoids at the 50% probability level. All hydrogens have been excluded for clarity except for the amide hydrogens.

Metal Complex Syntheses. All of the metal complexes are synthesized in ligand exchange reactions with either $Fe(acac)_3$ or $Ga(acac)_3$. These reactions proceed immediately upon the addition of base (KOH or Me_4NOH). Chromatographic purification (Sephadex LH-20, in MeOH) results in analytically pure metal complexes.

Description of the Structures of S-$\mathbf{1}_{Fe}(Me_4N)_3$ and S-$\mathbf{1}_{Ga}(Me_4N)_3$. The chemical and physical similarities of Fe^{III} and Ga^{III} are well documented,[19] and it is thus not surprising that the structures of $[Fe(S\text{-}(PhMe)_2TAM)_3](Me_4N)_3$, S-$\mathbf{1}_{Fe}(Me_4N)_3$, and $[Ga(S\text{-}(PhMe)_2TAM)_3](Me_4N)_3$, S-$\mathbf{1}_{Ga}(Me_4N)_3$, are isomorphic. The compounds crystallize in the cubic space group $I23$ with $Z = 8$, requiring the metal atoms to be positioned on a 3-fold axis. The asymmetric unit consists of one cation, one terephthalamide ligand, one molecule of MeOH, and one-third of a metal atom. Crystallographic data for both structures are presented in Table I with positional parameters comprising Table II (S-$\mathbf{1}_{Fe}$) and Table III (S-$\mathbf{1}_{Ga}$). ORTEP drawings of one-third of each of the anions are shown in Figure 2. The 2-fold symmetry of the terephthalamide ligand is not crystallographically imposed; however, the labeling scheme for the structures reflects the 2-fold symmetry of the free ligand with the numbering progressing outward from the terephthalamide carbons toward the chiral centers. The chemically related atoms are differentiated by A and B labels.[20] The isomorphic nature of the structures is immediately evident from the overlayed stereoview in Figure 3. The root-mean-square (rms) difference between the structures is 0.124 Å, with the greatest deviations occurring in the peripheral phenyl groups. A comparison of the catechol portion of the molecules shows a lesser rms difference of 0.047 Å. By comparison, the isomorphic $[Fe(catechol)_3]^{3-}$ and $[Ga(catechol)_3]^{3-}$ structures have an rms error of 0.061 Å.[21]

Tris-chelate metal complexes can exist as two coordination isomers, Δ or Λ, only one of which can be present in this space group ($I23$). The assignment of Λ at the metal center in both S-$\mathbf{1}_{Fe}$ and S-$\mathbf{1}_{Ga}$ proceeds directly from the assignment of the chirality at the methine carbon (S).[22]

The oxygen coordination environments at the metal centers have effective D_3 symmetry. The twist angle, which describes an O1A–M–O1B angle when these atoms are projected onto a plane perpendicular to the 3-fold axis, succinctly summarizes the slight differences in the coordination geometry. Twist angles of 41.5° and 43.8° are found for S-$\mathbf{1}_{Fe}$ and S-$\mathbf{1}_{Ga}$, respectively. The increase in the twist angle from Fe^{III} to Ga^{III} is consistent with an increase in the bite angle as predicted from simple repulsion calculations.[23] The bite angles of the terephthalamide oxygens, O1A–M–O1B, are 79.8° (S-$\mathbf{1}_{Fe}$) and 81.5(3)° (S-$\mathbf{1}_{Ga}$). A similar trend is found in other Fe^{III} and Ga^{III} tris(catecholate) structures[24-27] as shown in Table IV.

The absence of a crystallographic 2-fold axis in the structures of S-$\mathbf{1}_{Fe}$ and S-$\mathbf{1}_{Ga}$ requires a differentiation of the ends of each molecule when viewed down the 3-fold axis. For ease of comparison, the atoms in the upper portion of the molecules will be referred to with an A label and the lower a B label. The 3-fold related coordinating oxygens define two parallel planes perpendicular to the 3-fold axis: O1A/O1A′/O1A″ (P_{O1A}) and O1B/O1B′/O1B″ (P_{O1B}). The separation of these planes is 2.300 (S-$\mathbf{1}_{Fe}$) and 2.273 Å (S-$\mathbf{1}_{Ga}$) with the metal atoms nearly symmetrically disposed between them: [Fe–P_{O1A} (1.164 Å), Fe–P_{O1B} (1.136 Å)]; [Ga–P_{O1A} (1.167 Å), Ga–P_{O1B} (1.106 Å)]. The slight asymmetry is a manifestation of the differences in the metal oxygen distances in each structure with the metal oxygen bond of the upper portion (Fe–O1A, 2.020 Å; Ga–O1A, 1.993 Å) slightly longer than those of the lower (Fe–O1B, 1.999 Å; Ga–O1B 1.940 Å). The positioning of the metal atoms in S-$\mathbf{1}_{Fe}$ and S-$\mathbf{1}_{Ga}$ differs with respect to the least-squares plane of the central catechol ring, P_{AB}; both atoms are positioned out of P_{AB}, yet the iron is displaced to a much greater degree: 0.194 Å (S-$\mathbf{1}_{Fe}$); 0.023 Å (S-$\mathbf{1}_{Ga}$).

The greatest differentiation of the upper and lower portions of each structure occurs at the amide–aryl ring intersection. The angles between P_{AB} and the least-squares plane defined by each amide group, P_{AMA} and P_{AMB}, show similar trends in both structures (Table IV). The upper portions of the structures have a lesser twist (P_{AMA}–P_{AB}; 4° (S-$\mathbf{1}_{Fe}$); 2° (S-$\mathbf{1}_{Ga}$)) than the lower (P_{AMB}–P_{AB}; 15.4° (S-$\mathbf{1}_{Fe}$); 12° (S-$\mathbf{1}_{Ga}$)). In all cases, the amide proton is projected below P_{AB}[28] which allows for strong hydrogen bonding interactions between N1–H and O1; i.e. the metal–oxygen–hydrogen angle is more linear (Table IV).

The apparent visual 2-fold symmetry of the structures of S-$\mathbf{1}_{Fe}$ and S-$\mathbf{1}_{Ga}$ is enhanced by the seemingly symmetric disposition of the phenyl rings attached to the methine chiral centers above and below the central aryl ring (P_{AB}). The least-squares planes of these rings, P_A and P_B, intersect P_{AB} at similar angles in both S-$\mathbf{1}_{Fe}$ (130°, 123°) and S-$\mathbf{1}_{Ga}$ (128°, 124°).

Weakly Polar Interactions in S-$\mathbf{1}_{Fe}$ and S-$\mathbf{1}_{Ga}$. Theoretical analysis of the energetics of the benzene dimer indicates that the preferred structure in the gas phase is an edge–face orientation with a centroid–centroid distance of ca. 5 Å.[29] This conformation, in which there is a favorable interaction of the δ^+ H atom of one aromatic group with the δ^- π electron cloud of the other, is consistent with the results of a previous study of the benzene dimer.[30] In the optimum orientation the angle between the planes of the interacting aryl rings is ca. 90°.[29]

The aryl/aryl and alkyl/aryl interactions which stabilize the Λ isomer in S-$\mathbf{1}_{Fe}$ and S-$\mathbf{1}_{Ga}$ are easily seen in the solid state structures. The stereoview in Figure 4, which looks directly down

(19) Borgias, B. A.; Barclay, S. J.; Raymond, K. N. *J. Coord. Chem.* **1986**, *15*, 109.
(20) References to crystallographically threefold related atoms are designated with primes and double primes.
(21) (a) $[Fe(cat)_3]^{3-}$ crystal structure: Raymond, K. N.; Isied, S. S.; Brown, L. D.; Fronczek, F. R.; Nibert, J. H. *J. Am. Chem. Soc.* **1976**, *98*, 1767. (b) $[Ga(cat)_3]^{3-}$ crystal structure: see ref 19.
(22) No attempts were made to refine the other enantiomer.
(23) Kepert, D. L. In *Inorganic Stereochemistry*; Springer-Verlag: Heidelberg, 1982.
(24) Anderson, B. F.; Buckingham, D. A.; Robertson, G. B.; Webb, J.; Murray, K. S.; Clark, P. E. *Nature* **1976**, *262*, 722.
(25) Karpishin, T. B.; Stack, T. D. P.; Raymond, K. N. *J. Am. Chem. Soc.* **1993**, *115*, 182.
(26) Stack, T. D. P.; Raymond, K. N. Manuscript in preparation.
(27) Bulls, A. R.; Pippin, C. G.; Hahn, F. E.; Raymond, K. N. *J. Am. Chem. Soc.* **1990**, *112*, 2627.
(28) The position of the metal is arbitrarily taken as positive.
(29) Jorgensen, W. L.; Severance, D. L. *J. Am. Chem. Soc.* **1990**, *112*, 4768.
(30) Burley, S. K.; Petsko, G. A. *J. Am. Chem. Soc.* **1986**, *108*, 7995.

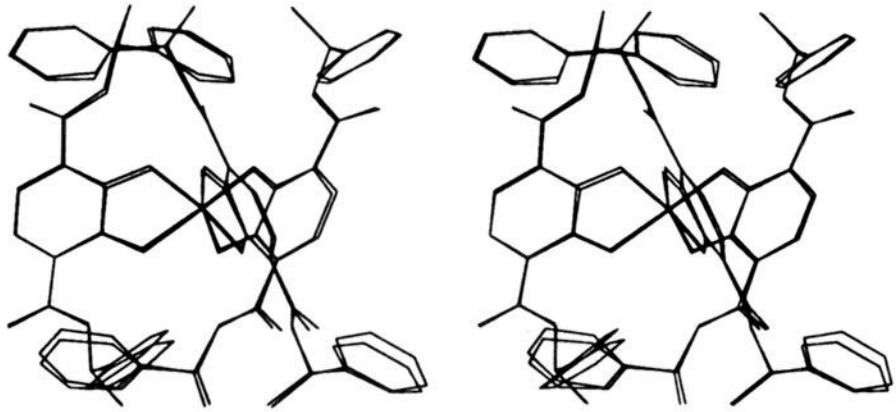

Figure 3. A stereoview of S-$\mathbf{1}_{Fe}$ and S-$\mathbf{1}_{Ga}$ overlayed. The root-mean-square deviation is 0.124 Å.

Table IV. Selected Metrical Data for S-$\mathbf{1}_{Fe}$ and S-$\mathbf{1}_{Ga}$ and Comparison of Tris(catecholate) Complexes

Coordination Geometry[a]

	O_{1A}–O_{1B} (Å)	bite[b]	M–O_{1A} (Å)	M–O_{1B} (Å)	C–O_{1A} (Å)	C–O_{1B} (Å)	O_{1A}–M–O_{1B} (deg)	M–P_{AB}[g] (Å)	O_{1A}–P_{AB} (Å)	O_{1B}–P_{AB} (Å)	P_{AB}–P_{OMO} (deg)	twist angle (deg)	ref
S-$\mathbf{1}_{Fe}$	2.58	1.28	2.020	1.999	1.31	1.32	79.8	0.194	0.001	0.041	6.5	41.5	this work
S-$\mathbf{1}_{Ga}$	2.57	1.31	1.943	1.994	1.30	1.31	81.5	0.023	0.045	0.006	2.0	43.8	this work
$[Fe(cat)_3]^{3-}$ [c,d]	2.62	1.30	2.017	2.012	1.34	1.33	81.3	0.145	0.019	–0.043	6.6	44.7	21a
$[Ga(cat)_3]^{3-}$ [c,d]	2.65	1.33	1.986	1.981	1.35	1.34	83.8	0.127	0.011	–0.044	6.1	48.8	19
$[Fe(cat)_3]^{3-}$ [c,e]	2.62	1.30	2.028	2.010	1.34	1.34	81.2	0.093	–0.019	0.009	4.6	46.5	24
$[Fe(eta)_3]^{3-}$ [c,d]	2.59	1.27	2.022	2.037	1.28	1.37	79.1	0.003	–0.102	–0.030	3.0	40.0	25
[Fe(bicapped trencam)]$^{3-}$ [c,f]	2.53	1.26	2.013	2.013	1.33	1.33	77.8	0.820	0.014	0.014	30.9	0.0	40

Hydrogen Bonding Interactions[a]

	P_{AMA}–P_{AB} (deg)	P_{AMB}–P_{AB} (deg)	O_{1A}–H_{N1A} (Å)	O_{1B}–H_{N1B} (Å)	O_{1A}–H_{N1A}–N_{1A} (deg)	O_{1B}–H_{N1B}–N_{1B} (deg)	M–O_{1A}–H_{N1A} (deg)	M–O_{1B}–H_{N1B} (deg)	ref
S-$\mathbf{1}_{Fe}$	+4.0	+15.4	1.80	1.85	137.6	133.6	145.9	146.6	this work
S-$\mathbf{1}_{Ga}$	+2.3	+12.4	1.77	1.86	138.5	134.4	147.1	145.1	this work
$[Fe(eta)_3]^{3-}$ [c,d]	+15.68	+4.38	1.77	1.80	133.5	131.7	145.5	139.4	25
[Fe(bicapped trencam)]$^{3-}$ [c,f]	+9.42	+9.42	1.80	1.80	135.8	135.8	137.6	137.6	40
$[Fe(eba)_3]^{3-}$ [c,d]	+8.37		1.77		133.7		145.1		26
[Fe(Trencam)]$^{3-}$ [c,d]	–16.00		1.95		127.1		130.00		18
[V(Trencam)]$^{3-}$ [c,d]	–16.20		1.98		123.7		127.9		27

[a] Definition of least-squares planes: P_{AB} [C1A,C2A,C3A,C1B,C2B,C3B]; P_A [C7A,C8A,C9A,C10A,C11A,C12A]; P_B [C7B,C8B,C9B,C10B,C11B,C12B]; P_{AMA} [C4A,O2A,N1A]; P_{AMB} [C4B,O2B,N1B]; P_{OMO} [O1A,M,O1B]. [b] Defined as $^1/_2(O_{1A}–O_{1B}/(M–O_{1A} + M–O_{1B}))$ or similarly 2 $\sin[^1/_2(O_{1A}–M–O_{1B})]$. [c] Abbreviation of ligands: cat = catecholate; eta = *N,N'*-diethyl-2,3-dihydroxyterephthalamide; eba = *N*-ethyl-2,3-dihydroxybenzamide; Trencam = tris(2-(2,3-dihydroxybenzamide) ethylamine. [d] Potassium salt. [e] Piperdinium salt. [f] Sodium salt. [g] The metal position is always considered above the plane.

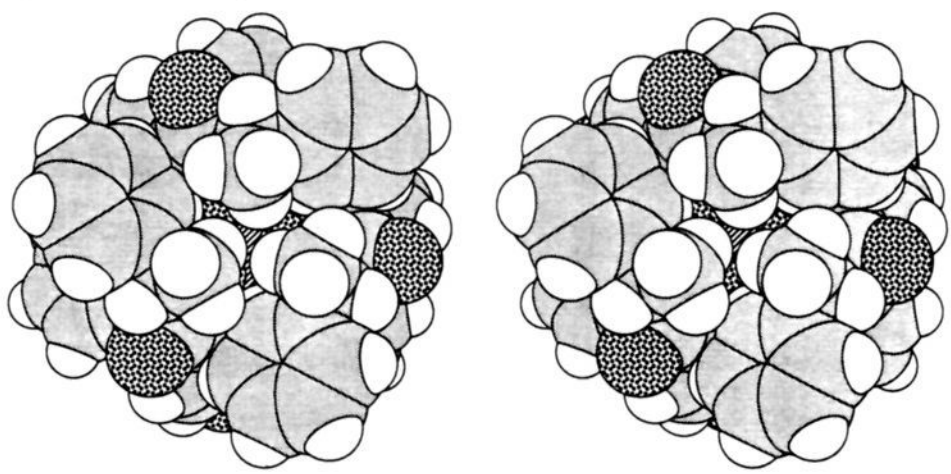

Figure 4. A space filling stereoview down the 3-fold axis of S-$\mathbf{1}_{Fe}$ showing the methyl/aryl interactions.

the 3-fold axis of S-$\mathbf{1}_{Fe}$, provides a clear view of three of the six methyl/aryl interactions operative in the complex. The α-methyl groups are projected toward the center of the peripheral phenyl rings and are on average 4.8 (S-$\mathbf{1}_{Fe}$) and 5.0 Å (S-$\mathbf{1}_{Ga}$) from the phenyl ring centroid.[31] In addition, geometrically favorable aryl/aryl interactions are developed between the peripheral phenyl groups and adjacent terephthalamide aryl rings. There are also six of these interactions per metal complex which can be most easily viewed in the stereo-sideview of Figure 3. Although the protons of the peripheral phenyl groups are not directed toward the center of the terephthalamide rings, the positioning is consistent with stabilizing aryl/aryl interactions observed in proteins.[30] The

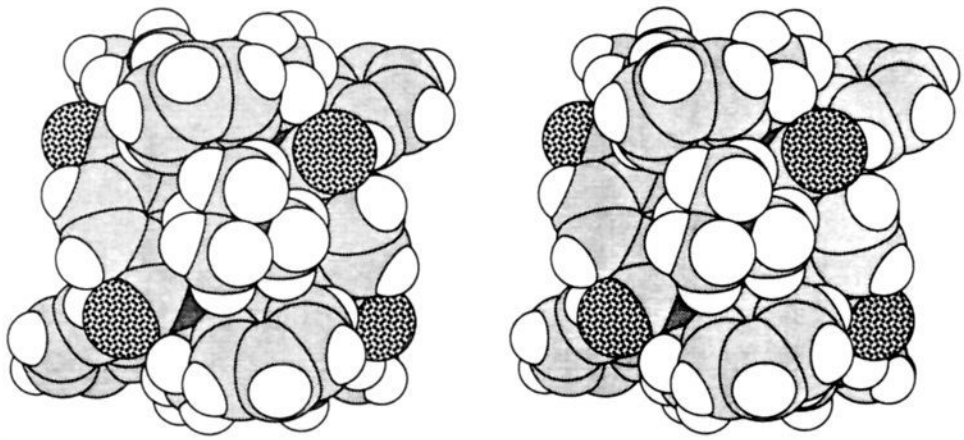

Figure 5. A space filling stereoview of S-$\mathbf{1}_{\mathbf{Fe}}$ showing the inclusion of one Me_4N^+ cation.

(average) centroid-to-centroid distances (5.4 ± 0.1 Å (S-$\mathbf{1}_{\mathbf{Fe}}$); 5.3 ± 0.1 Å (S-$\mathbf{1}_{\mathbf{Ga}}$)) and the aryl-plane to aryl-plane angles (83 ± 1° (S-$\mathbf{1}_{\mathbf{Fe}}$); 79 ± 1° (S-$\mathbf{1}_{\mathbf{Ga}}$)) describe enthalpically favorable geometries.

Three Me_4N^+ cations per complex anion are packed into the clefts formed between the terephthalamide rings. Each cation resides in a cavity capped on top and bottom by the phenyl rings $\mathbf{P_A}$ and $\mathbf{P_B}$ and on the sides by terephthalamide rings $\mathbf{P_{AB}}$ and $\mathbf{P_{AB'}}$, as shown in the space filling stereoview of Figure 5. This results in four weakly polar aryl–cation interactions with each Me_4N^+ cation. Although the positioning of the cations relative to the complex anion may first appear to be a consequence of compact crystal packing, ^1H NMR indicates that these aryl–cation interactions are operative in solution as well (see Discussion). The peripheral phenyl groups which define the top and bottom of a cavity do not arise from a single terephthalamide ligand and intersect at similar angles of 57.0° for S-$\mathbf{1}_{\mathbf{Fe}}$ and 60.9° for S-$\mathbf{1}_{\mathbf{Ga}}$. In both S-$\mathbf{1}_{\mathbf{Fe}}$ and S-$\mathbf{1}_{\mathbf{Ga}}$ the positively charged nitrogen is symmetrically disposed between the centroids of $\mathbf{P_A}$ and $\mathbf{P_B}$ at a distance of 4.6 Å and asymmetrically between the side terephthalamide ring centroids at 4.7 and 5.3 Å.

Circular Dichroism of the Fe^{III} Complexes. Each of the Fe^{III} tris(catecholate) complexes were examined by circular dichroism (CD) spectroscopy to determine the absolute configuration of the major coordination isomer in solution. The spectra were all recorded in degassed H_2O at pH 9 to ensure complete deprotonation of the metal–ligand complexes in solution.

No correlated structural and spectroscopic data exist for Fe^{III} tris(catecholate) complexes to allow an unambiguous assignment of the coordination isomers of such complexes. The original assignment of the absolute configuration of $\mathbf{Ent_{Fe}}$ as Δ was ultimately inferred from the solid state structure of $[Cr(oxalate)_3]^{3-}$ through a series of CD comparisons. The configuration of $\mathbf{Ent_{Cr}}$ was assigned as Δ by comparison of its CD spectrum with the spectra of the resolved isomers of $[Cr(catechol)_3]^{3-}$ which were assigned by comparison with the CD spectra of $[Cr(oxalate)_3]^{3-}$.[12a] A much more direct analysis is presented here to confirm that the configuration of $\mathbf{Ent_{Fe}}$ is indeed Δ. The crystal structure of S-$\mathbf{1}_{\mathbf{Fe}}$ shows unambiguously that the coordination isomer in the solid state is Λ. The solution CD spectra of S-$\mathbf{1}_{\mathbf{Fe}}$ and $\mathbf{Ent_{Fe}}$ in water are shown in Figure 6. The spectrum of S-$\mathbf{1}_{\mathbf{Fe}}$ has a positive band at 541 nm which is *opposite* to and almost equal in intensity to the band at 533 nm in $\mathbf{Ent_{Fe}}$. These bands arise from ligand-to-metal charge transfer (LMCT) transitions[32] and are therefore sensitive to the chirality at the metal center. These CD spectra

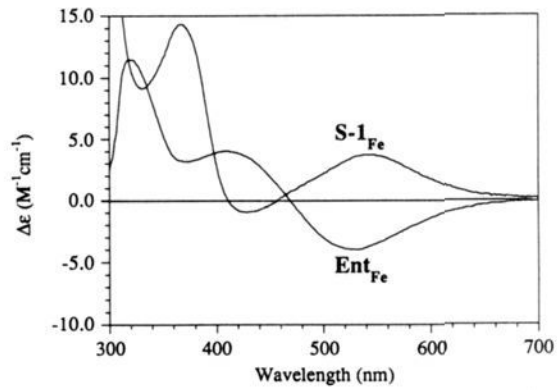

Figure 6. Circular dichroism spectra of $[Fe(S\text{-}(PhMe)_2TAM)_3]^{3-}$, S-$\mathbf{1}_{\mathbf{Fe}}$, and $[Fe(enterobactin)]^{3-}$, $\mathbf{Ent_{Fe}}$ (H_2O, pH 9).

allow the absolute configuration in $\mathbf{Ent_{Fe}}$ to be assigned as Δ (opposite to S-$\mathbf{1}_{\mathbf{Fe}}$). To correlate the solid state chirality of S-$\mathbf{1}_{\mathbf{Fe}}$ to the solution state, a solid state CD spectrum of a KBr pellet of X-ray quality crystals of S-$\mathbf{1}_{\mathbf{Fe}}(Me_4N)_3$ was recorded. The positive deflection of the band at 541 nm[33] indicates that the chirality at the metal center is unchanged between the solid and solution state. Thus, the coordination geometry in $\mathbf{Ent_{Fe}}$ must be Δ as previously assigned. In addition, the following spectroscopic evidence indicates that S-$\mathbf{1}_{\mathbf{Fe}}$ exists as essentially *100%* Δ in water: (1) the similar intensity of the 541-nm CD band to that observed for $\mathbf{Ent_{Fe}}$ (Figure 6); (2) small X-ray quality crystals of the complex S-$\mathbf{1}_{\mathbf{Fe}}K_3$, which also crystallizes in the noncentric space group $I23$, gave the same CD spectrum 2 min and 24 h after dissolution in H_2O, indicating that the complex does not racemize over that time period. It is impossible to assess, however, if a small degree of racemization occurs instantly upon dissolution. The complex S-$\mathbf{1}_{\mathbf{Fe}}(Me_4N)_3$, for which the crystal structure was obtained, could not be tested in a similar way in H_2O due to its insolubility.

The data for the CD spectra of all of the Fe^{III} complexes are presented in Table V (additional spectral data are contained in the Experimental Section). A clear correlation between the sign of the CD bands at ≈535 nm and the ligand chirality is maintained: with the R ligands, the major isomer is Δ, while with the S ligands it is Λ. This is in contrast to **Ent**, which has S chirality in the backbone, but results in the Δ isomer at the metal center. This difference is understandable if one considers the nature of the interactions involved. We have recently discussed that interactions *within* the trilactone backbone of **Ent** are responsible for the Δ chelation.[11] With the ligands in this study, however, *interligand* interactions which develop upon metal

(31) S-$\mathbf{1}_{\mathbf{Fe}}$: Me-Ph′: C6A′-centroid(C7A-C12A), 4.990 Å; Me-Ph′: C6B′-centroid(C7B-C12B), 4.756 Å; centroid($\mathbf{P_A}$)-centroid($\mathbf{P_{AB'}}$), 5.368 Å; centroid-($\mathbf{P_B}$)-centroid($\mathbf{P_{AB'}}$), 5.513 Å; S-$\mathbf{1}_{\mathbf{Ga}}$: Me-Ph′: C6A′-centroid(C7A-C12A), 5.279 Å; Me-Ph′: C6B′-centroid(C7B-C12B), 4.736 Å; centroid($\mathbf{P_A}$)-centroid-($\mathbf{P_{AB'}}$), 5.274 Å; centroid($\mathbf{P_B}$)-centroid($\mathbf{P_{AB'}}$), 5.432 Å.

(32) Karpishin, T. B.; Gebhard, M. S.; Solomon, E. I.; Raymond, K. N. *J. Am. Chem. Soc.* **1991**, *113*, 2977.

(33) The Δε value for this band was not determined in the KBr pellet since the dielectric constant of the KBr would be expected to influence the extinction coefficients of the charge transfer bands.

Table V. Circular Dichroism Results of the Fe^{III} Complexes in Water

complex	major diastereomer	λ_{max} (nm), $\Delta\epsilon$ (M^{-1} cm^{-1})
R-$\mathbf{5}_{Fe}$	Δ	535, −1.6
S-$\mathbf{5}_{Fe}$	Λ	535, +1.6
R-$\mathbf{4}_{Fe}$	Δ	535, −0.55
S-$\mathbf{3}_{Fe}$	Λ	536, +1.5
R-$\mathbf{2}_{Fe}$	Δ	542, −1.1
S-$\mathbf{1}_{Fe}$	Λ	541, +3.8
$\mathbf{Ent}_{Fe}$	Δ	533, −4.0

Table VI. ^1H NMR Results of the Ga^{III} Complexes

complex	diastereomer	% abundance (D_2O)
R-$\mathbf{4}_{Ga}$	Δ ↔ Λ	fast exchange
S-$\mathbf{3}_{Ga}$	Δ	14(1)[a]
	Λ	86(1)[a]
R-$\mathbf{2}_{Ga}$	Δ	85(1)[b]
	Λ	15(1)[b]
S-$\mathbf{1}_{Ga}$	Λ	100
$\mathbf{Ent}_{Ga}$	Δ	100

[a] Ten measurements between 5 and 95 °C. [b] Three independent measurements at 3 °C.

complexation effect stereoselectivity. Thus the inherent difference in the nature of the interactions precludes a specific comparison of the stereoselectivity seen in **Ent** complexes with the ones in this study.

The extent to which chirality has been induced in the Fe^{III} complexes can be determined qualitatively from the amplitude of the CD bands in the visible region. Quantitative measurements are problematic since CD spectroscopy is a difference measurement and small changes in the inherent $\Delta\epsilon$ intensities among the complexes can lead to significant apparent changes in the derived Δ:Λ ratios. In contrast, quantitative information can be obtained from ^1H NMR spectroscopy (*vide infra*). From the CD data in Table V, the trend that emerges is that both the number and nature of the chiral appendages are important in effecting stereoselectivity. The smallest degree of stereoselectivity is observed with TREN(EtMe)TAM, **4**. Doubling the number of chiral appendages in the metal complex of $(EtMe)_2$TAM, **2**, doubles the amplitude of the band at ≈540 nm, indicating a greater degree of stereoselective formation of one isomer. The Fe^{III} complexes of **3** and **5** both contain the same type (PhMe) and number (3) of chiral appendages yet their topologies are fundamentally different: $\mathbf{5}_{Fe}$ is a simple tris-chelate complex which can exist as either the *fac* or *mer* isomer, while $\mathbf{3}_{Fe}$ has all three chelates tethered together and is forced to coordinate as the *fac* isomer. The $\Delta\epsilon$ values for the two complexes, however, are almost identical. Assuming that significant stereoselectivity is only induced in the *fac* isomer (where there are three interactions between the chiral moieties versus only one in the *mer* isomer) suggests that $\mathbf{5}_{Fe}$ is predominately this isomer. Finally, as mentioned above, doubling the (PhMe) interactions (in going to ligand **1** from **5**) results in 100% stereoselective formation of the Λ isomer.

In contrast to the low-energy bands, the CD bands at higher energy (<390 nm) are ligand centered transitions (π–π^*)[32] and are indicative of the chirality in each of the ligands (Figure 6). The ligands with *S* chirality adjacent to the catecholamide moiety, including **Ent**, have a positive π–π^* CD band (≈335 nm for the catecholamides; ≈365 nm for the terephthalamides); the converse is true for the *R* ligands.

^1H NMR of the Ga^{III} Complexes. The ^1H NMR spectra of the diamagnetic gallium tris(catecholate) complexes were recorded in D_2O (pD = 9) to determine the relative abundance of the diastereomeric coordination isomers, the results of which are summarized in Table VI. The $[Ga((S\text{-PhMe})CAM)_3]^{3-}$ complex, S-$\mathbf{5}_{Ga}$, can potentially exist as four isomers: Δ-*fac*, Λ-*fac*, Δ-*mer*, and Λ-*mer*. The NMR spectra of this complex exhibit broad peaks throughout the temperature range studied (5–95 °C) yet

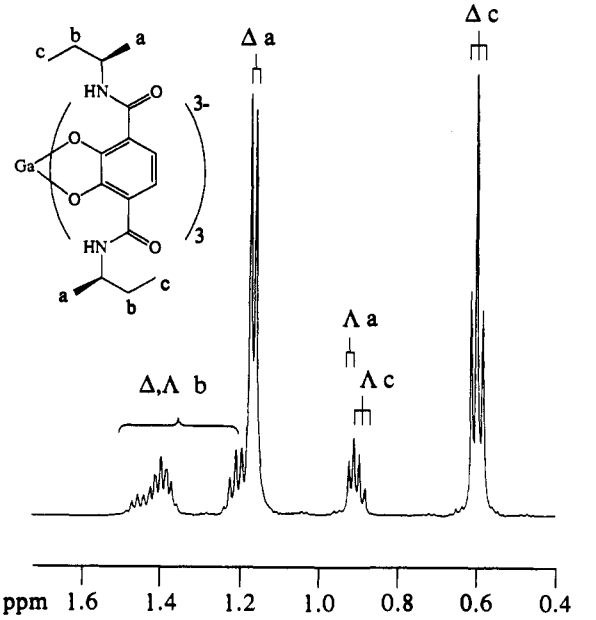

Figure 7. ^1H NMR spectrum of $[Ga(R\text{-}(EtMe)_2TAM)_3]^{3-}$, R-$\mathbf{2}_{Ga}$ (D_2O, 3 °C).

are indicative of only two species in solution. We assign these species as Λ-*fac* and Δ-*fac* based on the chemical shifts of the signals (*vide infra*) and the CD data for the related Fe^{III} complex; signal overlap prevented measurements of the diastereomer Λ:Δ ratio. The complex $[Ga(TREN(EtMe)TAM)]^{3-}$, $\mathbf{4}_{Ga}$, can only exist as the Δ-*fac* and Λ-*fac* isomers. At room temperature the spectrum of R-$\mathbf{4}_{Ga}$ shows only *one* set of broadened signals which sharpen significantly at 80 °C indicative of rapid exchange. The isomerization is slowed at 5 °C as indicated by the broadening of the signals. For the $[Ga(R\text{-}EtMe)_2TAM)_3]^{3-}$ complex, R-$\mathbf{2}_{Ga}$, the NMR spectrum at room temperature shows two sets of somewhat broadened signals which sharpen at 3 °C. The isomer interconversion (Δ ↔ Λ) at 3 °C is slow on the NMR time scale, allowing assignments and the isomer ratio to be determined. The resonance overlap in the δ 0.6–1.5 region required homonuclear decoupling for full assignments (Figure 7). The b-methylene protons are diastereotopic due to the adjacent chiral center, and there are thus four overlapping sextets (two for each isomer) in total for the b protons. The isomer ratio is 15:85 (Λ:Δ). The assignment of the favored isomer as Δ for the *R* ligands (and Λ for the *S* ligands) is based on the CD spectra of the Fe^{III} complexes (*vide supra*).

Total assignments of the protons in R-$\mathbf{2}_{Ga}$, in conjunction with the chemical shift dispersion caused by aromatic shielding effects, allows for a fair amount of structural information to be gleaned from the simple 1-D NMR spectrum. Assuming that in the favored Δ isomer the "a" methyl groups (Figure 7) are positioned in a similar fashion to that found for S-$\mathbf{1}_{Ga}$ (Figure 4), the "c" methyl protons will be positioned within the shielding cone of a neighboring terephthalamide ring, stabilized by the weakly polar electrostatic alkyl/aryl interactions. In the Λ isomer, however, the methyl "c" protons could not make a weakly polar interaction with an adjacent aryl group. This scenario should be indicated by the chemical shifts of the protons involved. In Figure 7, the chemical shift of the Δ-c protons is ≈0.3 ppm upfield from that of the Λ-c protons, consistent with these proposed interactions.

For $[Ga(S\text{-TREN}(PhMe)TAM)]^{3-}$, S-$\mathbf{3}_{Ga}$, at room temperature, the spectrum clearly shows two doublets for the methyl groups adjacent to the chiral centers (Figure 8a) and also two quartets for the protons at the chiral centers. The ratio Λ:Δ was determined to be 86:14, which does not vary over the temperature range 5–95 °C. Since the TREN protons display a similar coalescence behavior over the temperature range as in S-$\mathbf{4}_{Ga}$, this indicates that the cap is fluxional and that the isomers are

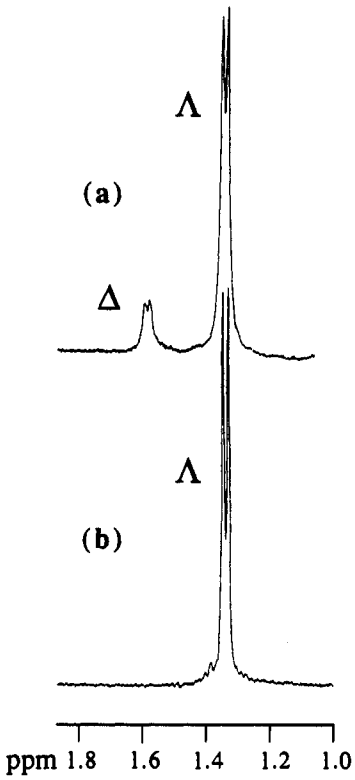

Figure 8. ^{1}H NMR spectra of the methyl region of: (a) [Ga(*S*-Tren(PhMe)TAM)]$^{3-}$, *S*-$\mathbf{3}_{Ga}$ and (b) [Ga(*S*-(PhMe)$_2$TAM)$_3$]$^{3-}$, *S*-$\mathbf{1}_{Ga}$ (D_2O, RT).

interconverting;[34] however, the expected temperature dependence of the isomer ratio was undetectable.

The ^{1}H NMR spectrum of [Ga(*S*-(PhMe)$_2$TAM)$_3$]$^{3-}$, *S*-$\mathbf{1}_{Ga}$, indicates a *single* isomer at room temperature in D_2O as found for $\mathbf{Ent}_{Ga}$. The similarity of the spectrum of X-ray quality crystals of the complex Λ-*S*-$\mathbf{1}_{Ga}(Me_4N)_3$ in $CDCl_3$ and that of polycrystalline *S*-$\mathbf{1}_{Ga}K_3$ in D_2O forces the conclusion that *S*-$\mathbf{1}_{Ga}$ exists solely as one isomer in aqueous solution. In addition, since the doublet assignable to the methyl group adjacent to the chiral center appears at exactly the same chemical shift as the methyl group of the Λ isomer in *S*-$\mathbf{3}_{Ga}$ (Figure 8), both signals must arise from the Λ isomer. It should be noted that the methyl group in the Δ isomer in *S*-$\mathbf{3}_{Ga}$ is at δ 1.60, which is very close to where the signal arises in the ligand by itself: δ 1.56 (D_2O, deprotonated pD = 13). The upfield shift of this methyl group in the Λ isomer of each of the complexes, *S*-$\mathbf{3}_{Ga}$ and *S*-$\mathbf{1}_{Ga}$, can be understood in examining the crystal structure of Λ-*S*-$\mathbf{1}_{Ga}$. In Figure 4, it is clear that the protons of the methyl groups are positioned within the shielding cone of a phenyl group on an adjacent ligand which would lead to this upfield shift. CPK molecular models suggest that in the Δ isomer the sterically demanding phenyl groups are rotated outward, thus removing this shielding effect.

Discussion

The Δ and Λ coordination isomers of tris-chelate metal complexes of chiral bidentate ligands are diastereomeric. This paper has shown that with the bidentate ligand *S*-(PhMe)$_2$TAM, *S*-**1**, essentially 100% formation of one isomer for its Fe^{III} and Ga^{III} complexes is observed in aqueous solution. The stereoselectivity in these complexes is effected by weakly polar interactions between adjacent ligands. The details of the interactions are elucidated by the solid state structures and confirmed to be operative in solution. This study represents the first demonstration of a bidentate ligand that results in 100% stereoselectivity in the formation of tris-chelate complexes with labile metal ions in aqueous solution.

(34) In a closely related complex with kinetically inert Rh^{III}, the TREN cap is static on the NMR time scale.

In examining the series of ligands in this study with regard to their stereoselectivities, the same trend is found for the series in both the Fe^{III} and Ga^{III} complexes: **4** < **2** < **5**, **3** < **1** (Table V and VI).[35] The ^{1}H NMR spectrum of $\mathbf{5}_{Ga}$ could not be definitively assigned, although from the CD spectrum of $\mathbf{5}_{Fe}$, the stereoselectivity of **5** is close to that of **3**. Both increasing the number of nonbonded interactions (**3** → **1** and **4** → **2**) and changing the substituents ethyl → phenyl result in a larger degree of stereoselectivity. The variation which has the larger effect is changing the ethyl groups in **2** and **4** to phenyl groups in **1** and **3** which results in favorable aryl/aryl and methyl/aryl interactions (*vide infra*).

Since *S*-$\mathbf{1}_{Ga}$ exists as essentially 100% Λ whereas the complex with half of the nonbonded interactions, *S*-$\mathbf{3}_{Ga}$, has a 86:14 Λ:Δ ratio (Figure 8), the free energy differences between the diastereomers can be determined for each of the complexes. The stabilization of the Λ isomer in *S*-$\mathbf{1}_{Ga}$ must be at least 2.7 kcal·mol^{-1} ($\Delta G = -RT \ln K$, 298 K, assuming 99:1 ratio) whereas in *S*-$\mathbf{3}_{Ga}$ it is 1.0 kcal·mol^{-1}. This nonlinear increase in the stereoselectivity from *S*-$\mathbf{3}_{Ga}$ to *S*-$\mathbf{1}_{Ga}$ may be due to a cooperativity between the top and bottom chiral appendages in *S*-$\mathbf{1}_{Ga}$. That is, the chiral interactions of one trigonal face dispose the other toward assembling in an analogous fashion, thus enhancing the same metal chirality. A similar cooperativity between the (EtMe) complexes *S*-$\mathbf{4}_{Ga}$ and *S*-$\mathbf{2}_{Ga}$ may also be operative; however, it could not be investigated since the diastereomeric distribution for *S*-$\mathbf{4}_{Ga}$ could not be measured.

The nonbonded weakly polar interactions that result in the stabilization of the Λ diastereomer for the complexes of *S*-**1** are illustrated in the isomorphic crystal structures of *S*-$\mathbf{1}_{Fe}$ and *S*-$\mathbf{1}_{Ga}$ (Figures 3–5). Both alkyl/aryl and aryl/aryl interactions are developed in the favored Λ isomer and are reduced upon isomerization (as indicated by CPK models). Comparison of the ^{1}H NMR spectra of *S*-$\mathbf{1}_{Ga}$ and *S*-$\mathbf{3}_{Ga}$ indicates that these interactions are operative in solution. Weakly polar alkyl/aryl interactions are also shown to result in stereoselectivity in the complexes of **2** and **4**. The stability gained in the formation of the weakly polar interactions can then be concluded to be the major driving force for the stereoselective chelation in these complexes. The magnitude of this enhanced stability (>2.7 kcal·mol^{-1} in *S*-$\mathbf{1}_{Fe}$ and *S*-$\mathbf{1}_{Ga}$) is commensurate with the aryl/aryl interaction of between 1 and 2 kcal mol^{-1} found for the energy (enthalpy) stabilization of a protein.[30]

In addition to stabilizing one diastereomer over the other, these weakly polar interactions are also capable of enhancing the overall stability of metal–ligand complexes in aqueous environments. Direct thermodynamic measurements of a family of [Fe^{III}(TAM)$_3$]$^{3-}$ complexes have been previously reported.[36] A noticable increase in the overall stability of the tris-chelate complex of the propyl TAM complex (log K_f = 43.2) is found relative to the methyl TAM complex (log K_f = 41.8). The propyl complex is capable of the identical alkyl/aryl interactions that are operative in the metal complexes of **2** and **4**, whereas these interactions are not possible in the methyl derivative.[37]

Since this study has focused on the effects of nonbonded interactions in water only, it is not clear how the stereoselectivity of these complexes will differ in various other solvents. A cursory

(35) The Fe^{III} and Ga^{III} complexes of ligands **2**, **3**, **4**, and **5** exist as a mixture of both Δ and Λ diastereomers in aqueous solution. Three pathways of interconversion of the diastereomers are possible: associative, dissociative, or intramolecular twisting: Serpone, N.; Bickley, D. G. *Prog. Inorg. Chem.* **1972**, *17*, 391.

(36) Garrett, T. M.; Miller, P. W.; Raymond, K. N. *Inorg. Chem.* **1989**, *28*, 128.

(37) The difference in the overall stability constants is primarily a result of an energetic difference in the formation of the tris-chelates from the bis-chelates. This is consistent with the fact that the entry of the third bidentate ligand results in the development of 4 of the 6 alkyl/aryl interactions. Weakly polar interactions thus provide an alternative explanation for the trends seen in the K_{130} values in ref 36.

(38) Abbreviations used in the text include the following: TREN, tris(2-aminoethyl)amine; s, singlet; d, doublet; t, triplet; qrt, quartet; q, quintet; sxt, sextet; m, multiplet; br, broad.

study in $CHCl_3$, however, indicates that both S-$\mathbf{1}_{Fe}$ and S-$\mathbf{1}_{Ga}$ (their Me_4N^+ salts) exist as 100% Λ with no loss in optical activity over days. The nonbonded interactions between the nonpolar moieties are not just a result of the need to exclude water from the periphery of the metal complex.

In addition to the aryl/aryl and methyl/aryl interactions, a similar weakly polar interaction involving the Me_4N^+ cations is observed in the crystal structures of S-$\mathbf{1}_{Fe}(Me_4N)_3$ and S-$\mathbf{1}_{Ga}$-$(Me_4N)_3$. Each Me_4N^+ resides in a cavity surrounded by four aryl rings (Figure 5). A similar structural arrangement in protic and aprotic solvents is indicated by ^1H NMR. The chemical shift of the Me_4N^+ protons in the Ga^{III} complex is at 2.05 ppm, whereas with free Me_4NOH in CD_3OD, the chemical shift is at 3.15 ppm. This provides evidence that even in methanol, each Me_4N^+ cation resides in this cavity of phenyl rings. The association of the cations with the complex anion is further corroborated by the solubility of S-$\mathbf{1}_{Ga}(Me_4N)_3$ and S-$\mathbf{1}_{Fe}(Me_4N)_3$ in $CHCl_3$, indicating that a tight ion aggregate is formed in solution. Recent studies have suggested that the interaction of the positively charged nitrogen of acetylcholine, ACh ($Me_3N^+(CH_2)_2OCOCH_3$), with the π systems of aryl rings at ACh binding sites is crucial for the recognition process.[3] It was previously believed that ACh must bind at an anionic site in acetylcholinesterase for example; however, the crystal structure of the enzyme[4] demonstrates that the binding site is actually a gorge lined with 14 aromatic residues, some of which must be involved in the binding and recognition of ACh.

Conclusions

This study has provided evidence to demonstrate the significance of weakly polar interactions in the stabilization of labile metal complexes. The structural characterizations of S-$\mathbf{1}_{Fe}$ and S-$\mathbf{1}_{Ga}$ provide a view of the interligand interactions that are operative in the series of complexes. In addition the structure of S-$\mathbf{1}_{Fe}$ combined with CD spectroscopy allows the chirality of $\mathbf{Ent}_{Fe}$ to be unambiguously assigned to the Δ isomer as previously reported. The aryl/aryl, alkyl/aryl, and cation/aryl interactions have been shown to not be attributable to crystal packing or hydrophobic effects (i.e. the exclusion of water). These interactions play a substantial role in biological recognition and protein structure and, within the framework of chiral ligands, can be instrumental in the stereoselective chelation of labile metal ions. As our knowledge and understanding of molecular interactions and recognition processes continue to expand, the design of weakly polar interactions into molecular hosts and catalysts will become increasingly important.

Experimental Section[38]

Physical Measurements. ^1H NMR spectra were measured at 298 K (except where specified differently) on a Bruker AM-500 or AM-400 spectrometer. Spectra recorded in D_2O (pD = 9) were referenced to 3-(trimethylsilyl)propionic-2,2,3,3-d_4 acid, sodium salt at $\delta = 0.00$ ppm. Absorption spectra were recorded on an HP 8450 UV–visible diode array spectrophotometer. CD spectra were collected on a JASCO J-500C spectropolarimeter equipped with an IF-500 II A/D converter. Crystal data were collected on an Enraf-Nonius CAD-4 diffractometer. Microanalyses were performed by the Analytical Services Laboratory, College of Chemistry, University of California, Berkeley. FAB mass spectra were performed at the Mass Spectrometry Laboratory, College of Chemistry, University of California, Berkeley.

Preparation of Compounds. All manipulations and operations were performed under Ar with dried solvents. Most of the metal complexes, however, showed no tendency to oxidize when exposed to oxygen over the course of days. The Ga^{III} and Fe^{III} complexes of **Ent** and **5** do oxidize slowly and were handled appropriately. The tetrahydrofuran was distilled from sodium benzophenone ketal. Dioxane was stored over activated 4 Å molecular sieves. TREN was distilled from sodium. All other compounds used were of reagent grade and were not further purified. The ligand precursors **A**, **B**, **C**, and **D** and [Ga(acac)$_3$] were prepared according to the published procedures.[25] The optical purity of the chiral amines was >99%.

Ligand Syntheses (see Scheme I). 2,3-Bis(benzyloxy)-1-((2-thioxothiazolidin-1-yl)carbonyl)benzene (F). 2,3-Bis(benzyloxy)benzoic acid was synthesized according to Shuda[39] except that the benzylation was performed in DMF. ^1H NMR (d_6-DMSO) δ 3.58 (s, OMe, 6H), 6.66 (s, ArH, 2H), 9.27 (s, OH, 2H). 2,3-Bis(benzyloxy)benzoic acid was pulverized and dried under vacuum at 100 °C. The dried solid (46 g, 137 mmol, 1.0 equiv) was added to 500 mL of dry CH_2Cl_2 with 31.22 g of N,N'-dicyclohexylcarbodiimide (DCC) (151 mmol, 1.1 equiv) and 0.6 g of 4-(dimethylamino)pyridine. The solids dissolved with stirring. With the addition of 2-mercaptothiazoline (16.4 g, 137 mmol, 1.0 equiv) the color changed to bright yellow and a white precipitate formed. The slurry was stirred overnight and the DC-urea was removed by filtration. The filtrate was washed with 0.5 M NaOH (3×), 1 M HCl (1×), and finally brine. After drying over $MgSO_4$, the CH_2Cl_2 solution was pushed through a flash-silica plug. After solvent removal, the residue was resuspended in ~200 mL of CH_2Cl_2 and filtered. The filtrate was layered with hexanes (~300 mL) and stored overnight at –20 °C. The yellow crystalline product (43.6 g, 72%) was collected in two crops. ^1H NMR ($CDCl_3$) δ 2.85 (t, CH_2N, 2H), 4.34 (t, CH_2S, 2H), 5.130 (s, OCH_2, 2H), 5.136 (s, OCH_2, 2H), 6.97 (dd, ArH, 1H), 7.09–7.07 (m, ArH, 2H). Elemental Anal. for $C_{24}H_{21}NO_3S_2$: calcd (found) C, 66.18 (65.85); H, 4.86 (4.74); N, 3.22 (3.23).

S-(PhMe)$_2$TAM-Me$_2$ (S-1Me$_2$). To a 200-mL CH_2Cl_2 solution of 5.82 g of **B** was added 5.62 g (46.5 mmol, 2.1 equiv) of (*S*)-α-methylbenzylamine and 2 mL of Et_3N at room temperature. The solution was stirred for 2 h and then diluted with 1 M HCl. The organic layer was separated and washed an additional time with 1 M HCl, followed by 1 M NaOH, and finally dried over $MgSO_4$. Removal of the CH_2Cl_2 left a white solid which was recrystallized from acetone at –20 °C to give 6.1 g (64%) of a fluffy white solid. ^1H NMR ($CDCl_3$) δ 1.59 (d, CH_3, 6H), 3.84 (s, OMe, 6H), 5.35 (qrt, CH, 2H), 7.27–7.40 (m, ArH, 10H), 7.92 (s, ArH, 2H), 8.14 (d, NH, 2H). Elemental Anal. for $C_{26}H_{28}O_4N_2$: calcd (found) C, 72.20 (71.95); H, 6.52 (6.73); N, 6.48 (6.80).

S-(PhMe)$_2$TAMH$_2$ (S-1). A large excess of BBr_3 (3.0 mL) was added in a single portion to a degassed CH_2Cl_2 solution of 4.1 g (9.48 mmol) of S-1Me$_2$ at 0 °C. The canary yellow slurry which resulted was stirred for 4 days at room temperature. The volatiles were removed under reduced pressure and water was carefully added. The mixture was heated to reflux which resulted in a solid yellow mass. After cooling, the solid material was dissolved in refluxing MeOH. Four cycles of dissolution followed by evaporation at 60 °C were sufficient to remove the borates. The remaining pale yellow material was recrystallized from CH_2Cl_2 as a colorless solid: 2.8 g (73%). ^1H NMR ($CDCl_3$) δ 1.62 (d, CH_3, 6H), 5.32 (q, CH, 2H), 7.26–7.38 (m, ArH, 10H), 7.05 (d, NH, 2H, J = 7.4 Hz), 7.11 (s, ArH, 2H), 10.82 (s, OH, 2H). Elemental Anal. for $C_{24}H_{24}O_4N_2$: calcd (found) C, 71.27 (71.15); H, 5.98 (6.11); N, 6.93 (7.17).

R-(EtMe)$_2$TAM-Bz$_2$ (R-2Bz$_2$). Compound **E**[40] (3.00 g, 5.24 mmol) was dissolved in 150 mL of CH_2Cl_2 and 1.10 mL (10.7 mmol) of (*R*)-*sec*-butylamine was added dropwise. The colorless solution was stirred at room temperature for 30 min, extracted with 0.1 M $KHCO_3$, dilute HCl, and dried ($MgSO_4$). The solution was taken to dryness to give 2.36 g of a white solid (92%). ^1H NMR ($CDCl_3$) δ 0.82 (t, CH_3, 6H), 0.99 (d, CH_3, 6H), 1.31 (m, CH_2, 4H), 4.01 (m, CH, 2H), 5.18 (dd, OCH_2, 4H), 7.39 (s, ArH, 10H), 7.58 (d, NH, 2H, J = 8.0 Hz), 7.98 (s, ArH, 2H).

R-(EtMe)$_2$TAMH$_2$ (R-2). To a solution of R-2Bz$_2$ (2.31 g, 4.73 mmol) in absolute EtOH was added 2 mL of glacial acetic acid and 0.350 g of 10% Pd/C catalyst. The solution was pressurized at 1500 psi H_2 in a stainless steel bomb and stirred at room temperature for 4 h. The solution was filtered through a Celite pad and the solvent removed. After coevaporation with C_6H_6 to remove the acetic acid, the brown solid was taken up in CH_2Cl_2 and filtered and the solvent removed to give 1.32 g of off-white crystalline material (90%). ^1H NMR ($CDCl_3$) δ 0.97 (t, CH_3, 6H), 1.26 (d, CH_3, 6H), 1.60 (m, CH_2, 4H), 4.13 (m, CH, 2H), 6.60 (d, NH, 2H, J = 7.7 Hz), 7.08 (s, ArH, 2H), 11.11 (s, OH, 2H). Elemental Anal. for $C_{16}H_{24}N_2O_4$: calcd (found) C, 62.32 (62.65); H, 7.84 (7.76); N, 9.08 (8.83).

(39) Schuda, P. F.; Botti, C. M.; Venuti, M. C. *OPPI Briefs* **1984**, *16*, 119.
(40) Garrett, T. M.; McMurry, T. J.; Hosseini, M. W.; Reyes, Z. E.; Hahn, F. E.; Raymond, K. N. *J. Am. Chem. Soc.* **1991**, *113*, 2965.
(41) H_6(enterobactin)·H_2O was isolated from cultures of *E. coli* AN311 as previously described: Young, I. G.; Gibson, F. *Methods Enzymol.* **1979**, *56*, 394.
(42) The ^1H NMR spectrum of $\mathbf{Ent}_{Ga}$ in d_6-DMSO has previously been published: Llinás, M.; Wilson, D. M.; Neilands, J. B. *Biochemistry* **1973**, *12*, 3836.

S-TREN(PhMe)TAM-Me$_6$ (S-3Me$_6$). Compound **D** (1.00 g, 0.931 mmol) was dissolved in 40 mL of $CHCl_3$ and 0.367 mL of (*S*)-α-methylbenzylamine (2.88 mmol) was added. After the mixture was stirred for 6 days at room temperature, the yellow color had disappeared. The solution was extracted with 0.2 M NaOH and dried ($MgSO_4$) before the solvent was removed to an oily white solid. The product was purified on a flash silica column (1–3% MeOH/CH_2Cl_2) to yield a colorless microcrystalline material (0.81 g, 81%). ^{1}H NMR ($CDCl_3$) δ 1.62 (d, CH_3, 9H), 2.86 (t, CH_2, 6H), 3.59 (qrt, CH_2, 6H), 3.80 (s, OCH_3, 9H), 3.91 (s, OCH_3, 9H), 5.33 (m, CH, 3H), 7.26–7.41 (m, ArH, 15H), 7.67 (s, ArH, 6H), 8.03 (t, NH, 3H), 8.20 (d, NH, 3H, J = 7.9 Hz).

S-TREN(PhMe)TAMH$_6$·HBr (S-3·HBr). *S*-3Me$_6$ (0.81 g, 0.75 mmol) was dissolved in 40 mL of CH_2Cl_2 and blanketed with Ar and 4.0 mL of BBr_3 was added. The yellow suspension was stirred at room temperature under Ar for 5 days. The mixture was taken to dryness and coevaporated with MeOH 10 times. The brown solid was taken up in acetone and precipitated with Et_2O to give an off-white solid (0.64 g, 79%). ^{1}H NMR (d_6-DMSO) δ 1.51 (d, CH_3, 9H), 3.53 (br t, CH_2, 6H), 3.74 (br qrt, CH_2, 6H), 5.19 (m, CH, 3H), 7.22–7.51 (m, ArH, 21H), 9.06 (br t, NH, 3H), 9.17 (d, NH, 3H, J = 7.8 Hz), 9.66 (br t, NH, 1H), 12.06 (s, OH, 3H), 12.77 (s, OH, 3H). ^{1}H NMR (D_2O; pD 13) δ 1.56 (d, CH_3, 9H), 2.96 (br t, CH_2, 6H), 3.64 (br qrt, CH_2, 6H), 5.10 (m, CH, 3H), 6.97 (s, ArH, 6H), 7.45 (m, ArH, 15H). Elemental Anal. for $C_{54}H_{58}N_7O_{12}Br$: calcd (found) C, 60.22 (60.49); H, 5.43 (5.74); N, 9.10 (9.24).

R-TREN(EtMe)TAM-Me$_6$ (R-4Me$_6$). Compound **D** (1.00 g, 0.931 mmol) was dissolved in 150 mL of CH_2Cl_2 and 0.350 mL of (*R*)-*sec*-butylamine (3.41 mmol) was added. The solution was stirred at reflux for 12 h and then extracted with 0.1 M KOH and dried ($MgSO_4$) before the solvent was removed to a white solid (0.737 g, 85%). No further purification was performed. ^{1}H NMR ($CDCl_3$) δ 0.99 (t, CH_3, 9H), 1.25 (d, CH_3, 9H), 1.61 (m, CH_2, 6H), 2.88 (t, CH_2, 6H), 3.61 (q, CH_2, 6H), 3.87 (s, OCH_3, 9H), 3.93 (s, OCH_3, 9H), 4.14 (m, CH, 3H), 7.67 (d, NH, 3H, J = 8.3 Hz), 7.70 (s, ArH, 6H), 8.06 (t, NH, 3H).

R-TREN(EtMe)TAMH$_6$·HBr (R-4·HBr). *R*-4Me$_6$ (0.50 g, 0.53 mmol) was dissolved in 30 mL of CH_2Cl_2 and blanketed with Ar and 2.0 mL of BBr_3 was added. The yellow suspension was stirred at room temperature under Ar for 70 h. The mixture was taken to dryness and coevaporated with MeOH 8 times. The beige solid was taken up in acetone and precipitated with Et_2O to give an off-white solid (0.48 g; 97%). ^{1}H NMR (d_6-DMSO) δ 0.87 (t, CH_3, 9H), 1.17 (d, CH_3, 9H), 1.55 (m, CH_2, 6H), 3.54 (br t, CH_2, 6H), 3.76 (br qrt, CH_2, 6H), 7.36 (dd, ArH, 6H), 8.57 (d, NH, 3H, J = 8.1 Hz), 9.04 (br t, NH, 3H), 9.66 (br t, NH, 1H), 12.00 (s, OH, 3H), 13.07 (s, OH, 3H). Elemental Anal. for $C_{42}H_{57}N_7O_{12}$·HBr·H_2O: calcd (found) C, 53.05 (53.19); H, 6.36 (6.18); N, 10.31 (9.95).

***R*- and *S*-(PhMe)CAM-Bz$_2$ (*R*- and *S*-5Bz$_2$).** Preparation of the *S* isomer is analogous to the following. To a 30-mL CH_2Cl_2 solution of compound **F** (2.50 g, 5.74 mmol) was added 850 μL of *R*(+)-α-methylbenzylamine (6.28 mmol). The solution was stirred at reflux for 4 h until all of the yellow color due to compound **F** had disappeared. The solution was extracted with 0.2 M NaOH and dilute HCl, followed by drying ($MgSO_4$) and solvent removal to yield a colorless viscous oil (2.49 g, 99%). ^{1}H NMR ($CDCl_3$) δ 1.34 (d, CH_3, 3H), 5.03 (dd, 2-OCH_2, 2H), 5.14 (s, 3-OCH_2, 2H), 5.24 (m, CH, 1H), 7.14–7.77 (m, ArH, 18H), 8.33 (d, NH, 1H). Elemental Anal. for $C_{29}H_{27}NO_3$: calcd (found) C, 79.61 (79.28); H, 6.22 (5.98); N, 3.20 (2.70).

***R*- and *S*-(PhMe)CAMH$_2$ (*R*- and *S*-5).** Preparation of the *S* isomer is analogous to the following. To a solution of compound *R*-5Bz$_2$ (2.50 g, 5.71 mmol) in absolute EtOH was added 2 mL of glacial acetic acid and 0.350 g of 10% Pd/C catalyst. The solution was pressurized at 1500 psi H_2 in a stainless steel bomb and stirred at room temperature overnight. The ethanolic solution was filtered through a Celite pad and the solvent removed. After coevaporation with C_6H_6 to remove the acetic acid, the oily solid was taken up in acetone and precipitated with Et_2O to give an off-white crystalline material. ^{1}H NMR (d_6-DMSO) δ 1.48 (d, CH_3, 3H), 5.18 (m, CH, 1H), 6.63 (t, ArH, 1H), 6.88 (d, ArH, 1H), 7.2–7.42 (m, ArH, 6H), 9.30 (d, NH, 1H, J = 7.5 Hz). Elemental Anal. for $C_{15}H_{15}NO_3$: calcd (found) C, 70.02 (69.81); H, 5.88 (5.80); N, 5.44 (5.71).

Metal Complex Syntheses. Ent$_{Fe}$K$_3$. To a degassed MeOH solution of H_6(enterobactin)·H_2O[41] (0.033 g; 0.048 mmol) was added a solution of Fe(acac)$_3$ in degassed MeOH (0.048 mmol). The solution immediately turned black/red. A KOH solution in MeOH (0.144 mmol) was then added via cannula and the solution turned deep red. The solution was taken to dryness and applied to a BIOGEL P-2 column in water in an inert atmosphere box. The Ent$_{Fe}$K$_3$ complex eluted as a single red band, which was dried in vacuo (80 °C) and stored under Ar. Elemental Anal. for $K_3FeC_{30}H_{21}N_3O_{15}$: calcd (found) C, 43.01 (43.40); H, 2.53 (2.71); N, 5.02 (4.80). UV–vis (H_2O, pH 9; λ (nm), ε (M^{-1} cm^{-1})) 494, 5400. CD (H_2O, pH 9; λ (nm), Δε (M^{-1} cm^{-1})) 320, +11.5; 409, +4.0; 533, –4.0.

Ent$_{Ga}$K$_3$ was prepared in a similar fashion to **Ent$_{Fe}$K$_3$** using Ga(acac)$_3$. ^{1}H NMR (D_2O)[42] δ 3.97 (dd, $C_\beta H_1$, 3H, $J_{\beta\beta}$ = 11.9 Hz, $J_{\beta\alpha}$ = 2.2 Hz), 5.24 (t, $C_\alpha H$, 3H, $J_{\alpha\beta}$ = 2.3 Hz), 5.48 (dd, $C_\beta H_2$, 3H, $J_{\beta\beta}$ = 11.9 Hz, $J_{\beta\alpha}$ = 2.4 Hz), 6.56 (t, ArH_m, 3H, J = 7.8 Hz), 6.77 (dd, ArH, 3H, J_1 = 7.5 Hz, J_2 = 1.6 Hz), 7.08 (dd, ArH, 3H, J_1 = 8.2 Hz, J_2 = 1.6 Hz).

***S*-1$_{Fe}$(Me$_4$N)$_3$.** To a degassed MeOH solution of *S*-**1** (0.170 g, 0.43 mmol, 3 equiv) was added 0.050 g of Fe(acac)$_3$ and 0.077 g (0.43 mmol, 3 equiv) of $Me_4NOH·5H_2O$ as solids. The solution was heated to reflux under an Ar flow during which time the solution changed color to the characteristic Fe^{III} tris-catecholate red. The solvent was removed and the remaining solid was gently heated under vacuum to remove the remaining acacH. The solid was resuspended in 10 mL of MeOH to which 0.013 g (0.5 equiv) of $Me_4NOH·5H_2O$ had been added. After layering diethyl ether (20 mL), the solution was stored at –20 °C overnight. Black crystalline material was collected, washed with Et_2O, and dried under vacuum to yield 0.20 g (65%) of pure product. MS-FAB (3-NBA) MH^+ 1486.2 (exact mass, 1484.7). Elemental Anal. for $FeC_{84}H_{102}N_9O_{12}$: calcd (found) C, 67.91 (67.42); H, 6.92 (7.03); N, 8.49 (8.45).

***S*-1$_{Ga}$(Me$_4$N)$_3$** was synthesized in a similar fashion to *S*-**1$_{Fe}$**(Me$_4$N)$_3$ using Ga(acac)$_3$. MS-FAB (3-NBA) MH^+ 1499.4 (exact mass, 1497.7). Elemental Anal. for $GaC_{84}H_{102}N_9O_{12}·6H_2O$: calcd (found) C, 62.76 (63.24); H, 7.15 (7.03); N, 7.84 (7.61). ^{1}H NMR (CD_3OD) δ 1.28 (d, CH_3, 18H), 2.05 (s, Me_4N, 36H), 5.15 (qrt, CH, 6H), 7.19 (dd, ArH_m, 12H), 7.07–6.96 (m, ArH_o+Ar_p, 18H), 7.07 (s, ArH, 6H), 12.26 (d, NH, 6H). ^{13}C NMR (CD_3OD) δ 26.3, 55.3, 113.9, 115.9, 127.4, 128.1, 130.2, 146.0, 160.3, 170.3. ^{1}H NMR ($CDCl_3$) δ 1.41 (d, CH_3, 18H), 1.65 (s, Me_4N, 36H), 5.42 (qrt, CH, 6H), 7.36 (d, ArH_m, 12H), 7.11–7.06 (m, ArH_o+ArH_p, 18H), 7.30 (s, ArH, 6H), 11.92 (d, NH, J = 9.8 Hz, 6H). ^{13}C NMR ($CDCl_3$) δ 25.7, 48.2, 54.7, 113.3, 115.4, 126.7, 127.1, 129.1, 145.6, 158.0, 167.9.

***S*-1$_{Ga}$K$_3$.** To a degassed MeOH solution of *S*-**1** (0.100 g, 0.25 mmol, 3 equiv) was added 0.030 g of Ga(acac)$_3$ and 2.70 mL of 0.0989 M KOH (3.2 equiv) solution. The solution was heated to reflux under an Ar flow until most of the solvent was removed. The remaining residue was dried under vacuum with gentle heating. The solid was resuspended in 10 mL of acetone by heating. Cooling the solution to –20 °C overnight gave 0.040 g (32%) of prismatic crystals. ^{1}H NMR (D_2O, 2 weeks) δ 1.34 (d, CH_3, 18H), 5.09 (qrt, CH, 6H), 7.04 (s, ArH, 6H), 7.05 (t, ArH_o, 12H), 7.14 (t, Ar-H_p, 6H), 7.15 (d, Ar-H_m, 12H).

***S*-1$_{Fe}$K$_3$** was synthesized and crystallized in a similar fashion to *S*-**1$_{Ga}$**K$_3$ using Fe(acac)$_3$. Elemental Anal. for $K_3FeC_{72}H_{66}N_6O_{12}·2H_2O$: calcd (found) C, 61.05 (61.30); H, 4.98 (4.66); N, 5.93 (5.55). UV–vis (H_2O, pH 9; λ (nm), ε (M^{-1} cm^{-1})) 448, 6000. CD (H_2O, pH 9; λ (nm), Δε (M^{-1} cm^{-1})) 366, +14.3; 426, –0.94; 541, +3.8.

***R*-2$_{Fe}$K$_3$.** To 0.200 g of *R*-**2** (0.65 mmol) in degassed MeOH was added Fe(acac)$_3$ (0.076 g, 0.215 mmol). A solution of KOH in EtOH (0.5 M, 1.30 mL) was added and the solution turned deep red. The solution was taken to dryness and applied to a Sephadex LH-20 column in MeOH and the deep red band collected and dried to yield 0.200 g of black/red solid (85%). Elemental Anal. for $K_3FeC_{48}H_{66}N_6O_{12}·2H_2O$: calcd (found) C, 51.10 (50.77); H, 6.25 (6.18); N, 7.45 (7.69). UV–vis (H_2O, pH 9; λ (nm), ε (M^{-1} cm^{-1})) 448, 5600. CD (H_2O, pH 9; λ (nm), Δε (M^{-1} cm^{-1})) 365, –2.0; 425, +3.3; 542, –1.1.

***R*-2$_{Ga}$K$_3$** was synthesized in a similar fashion to *R*-**2$_{Fe}$**K$_3$ using Ga(acac)$_3$. Elemental Anal. for $K_3GaC_{48}H_{66}N_6O_{12}·3H_2O$: calcd (found) C, 49.69 (49.67); H, 6.26 (6.11); N, 7.24 (6.95). ^{1}H NMR (D_2O, 276 K) Δ isomer: δ 0.61 (t, CH_2-CH_3), 1.17 (d, CH-CH_3), 1.21 (m, CH_2-CH_3), 1.41 (m, CH_2-CH_3), 3.85 (sxt, CH-CH_3), 7.00 (s, Ar-H). ^{1}H NMR (D_2O, 276 K) Λ isomer: δ 0.90 (t, CH_2-CH_3), 0.92 (d, CH-CH_3), 1.21 (m, CH_2-CH_3), 1.46 (m, CH_2-CH_3), 3.82 (sxt, CH-CH_3), 7.00 (s, Ar-H).

***S*-3$_{Fe}$K$_3$.** To 0.150 g of *S*-**3**·HBr (0.14 mmol) in degassed MeOH was added 0.050 g of Fe(acac)$_3$ (0.14 mmol) and 4 equiv of KOH as an EtOH solution. The solution was taken to dryness and applied to a Sephadex LH-20 column in MeOH. The deep red band separated from a beige band on the column and was taken to dryness to give a black/red microcrystalline solid. Elemental Anal. for $K_3FeC_{54}H_{51}N_7O_{12}·7H_2O$: calcd (found) C, 50.31 (49.91); H, 5.08 (4.87); N, 7.60 (7.59). UV–vis (H_2O, pH 9; λ (nm), ε (M^{-1} cm^{-1})) 444, 5900. CD (H_2O, pH 9; λ (nm), Δε (M^{-1} cm^{-1})) 415, –1.4; 536, +1.5.

***S*-3$_{Ga}$K$_3$** was synthesized in a similar fashion to *S*-**3$_{Fe}$**K$_3$ using Ga(acac)$_3$. Elemental Anal. for $K_3GaC_{54}H_{51}N_7O_{12}·3H_2O$: calcd (found) C, 52.68

(52.56); H, 4.67 (4.50); N, 7.96 (7.84). ^{1}H NMR (D_2O, 298 K) Λ isomer: δ 1.34 (d, CH_3), 2.44 (br m, NCH), 2.61 (br m, NCH), 3.20 (br m, NCH), 3.71 (br m, NCH), 5.12 (qrt, CH), 7.0–7.6 (m, arom). ^{1}H NMR (D_2O, 298 K) Δ isomer: δ 1.60 (d, CH_3), 2.44 (br m, CH_2-TREN), 2.61 (br m, CH_2-TREN), 3.20 (br m, NCH), 3.71 (br m, NCH), 5.21 (qrt, CH), 7.0–7.6 (m, arom).

***R*-$4_{Fe}K_3$.** To 0.100 g of *R*-**4**·HBr (0.107 mmol) in degassed MeOH was added 0.038 g of $Fe(acac)_3$ and 4 equiv of KOH as an EtOH solution. Purification was the same as for *S*-$3_{Fe}K_3$. Elemental Anal. for $K_3FeC_{42}H_{51}N_7O_{12}\cdot 3H_2O$: calcd (found) C, 47.01 (47.30); H, 5.35 (5.17); N, 9.14 (8.94). UV–vis (H_2O, pH 9; λ (nm), ε (M^{-1} cm^{-1})) 448, 6200. CD (H_2O, pH 9; λ (nm), Δε (M^{-1} cm^{-1})) 395, +1.0; 535, –0.55.

***R*-$4_{Ga}K_3$** was synthesized in a similar fashion to *R*-$4_{Fe}K_3$ using $Ga(acac)_3$. Elemental Anal. for $K_3GaC_{42}H_{51}N_7O_{12}\cdot 3H_2O$; calcd (found) C, 46.41 (46.48); H, 5.29 (5.16); N, 9.02 (8.72). ^{1}H NMR (D_2O, 353 K) Δ and Λ isomers rapidly interconvert; δ 0.91 (t, CH_2-CH_3, 9H), 1.24 (d, CH-CH_3, 9H), 1.60 (q, CH_2-CH_3, 6H), 2.53 (br m, CH_2-TREN, 6H), 3.39 (br m, CH_2-TREN, 3H), 3.52 (br m, CH_2-TREN, 3H), 3.95 (sxt, CH-CH_3, 3H), 7.00 (dd, Ar-H, 6H).

***R*-$5_{Fe}K_3$.** To 0.16 g (0.62 mmol) of *R*-**5** in degassed MeOH was added 0.073 g (0.21 mmol) of $Fe(acac)_3$ and 3.5 equiv of KOH as an EtOH solution. The solution was taken to dryness and applied to a Sephadex LH-20 column in MeOH. The deep red band separated from a purple band on the column and was taken to dryness to give a brick red solid. Elemental Anal. for $K_3FeC_{45}H_{39}N_3O_9\cdot 2H_2O$: calcd (found) C, 55.44 (55.24); H, 4.45 (4.39); N, 4.31 (4.11). UV–vis (H_2O, pH 9; λ (nm), ε (M^{-1} cm^{-1})) 494, 3900. CD (H_2O, pH 9; λ (nm), Δε (M^{-1} cm^{-1})) 335, –11.1; 535, –1.6.

***S*-$5_{Fe}K_3$** was synthesized in a similar fashion to *R*-5_{Fe}. Elemental Anal. for $K_3FeC_{45}H_{39}N_3O_9\cdot 3.5H_2O$: calcd (found) C, 53.94 (53.89); H, 4.63 (4.59); N, 4.19 (4.21). UV–vis (H_2O, pH 9; λ (nm), ε (M^{-1} cm^{-1})) 494, 3900. CD (H_2O, pH 9; λ (nm), Δε (M^{-1} cm^{-1})) 335, +10.9; 535, +1.6.

***S*-$5_{Ga}K_3$** was synthesized in a similar fashion to *R*-5_{Fe} using $Ga(acac)_3$. Elemental Anal. for $K_3GaC_{45}H_{39}N_3O_9\cdot 2H_2O$: calcd (found) C, 54.66 (54.92); H, 4.38 (4.59); N, 4.25 (4.41).

Collection of X-ray Data for *S*-$1_{Fe}(Me_4N)_3$ and *S*-$1_{Ga}(Me_4N)_3$. X-ray quality crystals of both *S*-$1_{Fe}(Me_4N)_3$ and *S*-$1_{Ga}(Me_4N)_3$ were grown from a methanolic solution at room temperature which had been layered with Et_2O. Oil mounted, low-temperature structures were performed to minimize solvent loss. Unit cell and orientation matrix parameters were obtained from 24 machine-centered reflections with $20° < 2\theta < 24°$. Body-centered cubic cells with $m3$ Laue symmetry were suggested by TRACER (a subprogram of MolEN[43]) and supported by the high-angle unit-cell parameters. A unique forty-eighth of the Ewald sphere was collected by examining a unique octant, $+h$, $+k$, $+l$, and excluding reflections, $h + k + l = 2n + 1$ (body centering) and $l < k$ or $l < h$ (3-fold symmetry). Data collection and crystal parameters for both structures are found in the Table I. Three intensity check reflections monitored every hour of X-ray exposure exhibited no significant decay. Examination of suitable reflection intensities indicated that the crystals had $m3$ Laue symmetry rather than $m3m$. The molecular formulas in conjunction with volume calculations indicated $Z = 8$ with appreciable solvent inclusion.

Data Reduction, Solution, and Refinement of *S*-$1_{Fe}(Me_4N)_3$ and *S*-$1_{Ga}(Me_4N)_3$. The data were processed and the structures were refined using MolEN.[43] Atom scattering factors were taken from the tabulations of Cromer and Waber.[44] Lorentz and polarization corrections were applied; an absorption correction was deemed necessary by examination of ψ-scan data and an empirical correction was applied for both structures. The body-centering, along with the lack of a mirror plane perpendicular to the 110 or 101 or 011 axes,[45] restricted the choice of space groups to $I23$ or $I2_13$. Chirality of the ligand, in addition to the simple E statistics in MULTAN,[46] supported these noncentrosymmetric space groups. The metal–metal vectors in the Patterson maps proved to be consistent with space group $I23$.

Isotropic refinement with the inclusion of one MeOH molecule converged at R_w = 10.2% (*S*-1_{Fe}), 11.2% (*S*-1_{Ga}). The stereochemistry at the methine carbon was set to *S* which unambiguously defines the chirality at the metal center to be Λ in both structures. The Ga and Fe atoms were found not to be equivalently positioned in the asymmetric unit. A 90° rotation of the original data for *S*-1_{Ga} positioned the metals isomorphically assuring equivalent views down the polar 3-fold axis. All non-hydrogen atoms were refined anisotropically except for those of the solvent. The hydrogens were included at calculated positions, 0.95 Å from their parent atoms, for least-squares refinements. The hydrogen isotropic thermal parameters were set at 1.3 times the isotropic thermal parameter of the parent atom. For metrical calculations, the hydrogens were included at 1.08 Å for C–H bonds and 1.00 Å for amide protons.[47] The MeOH solvate in *S*-1_{Fe} was found to be disordered over two sites at a 60/40 occupancy while in *S*-1_{Ga} it was modeled at a single site with significant thermal motion.

Acknowledgment. This research was supported by National Institutes of Health Grant AI 11744. T.D.P.S. thanks the National Science Foundation for a postdoctoral fellowship 1988–1990 (CHE-8809111).

Supplementary Material Available: X-ray crystallographic data for *S*-1_{Fe} and *S*-1_{Ga}, including tables of anisotropic thermal parameters, hydrogen positional parameters, intramolecular distances, intramolecular angles, and intramolecular torsional angles (10 pages); listing of observed and calculated structure factors (30 pages). Ordering information is given on any current masthead page.

(43) MolEN: Molecular Structure Solution Procedures, Enraf-Nonius, 1990.

(44) Cromer, D. T.; Waber, J. T. *International Tables for X-ray Crystallography*; Kynoch Press: Birmingham, England, 1974; Vol. IV.

(45) $m3m$ Laue symmetry.

(46) MULTAN, A System of Computer Programs for Automatic Solution of Crystals Structures from X-ray Diffraction Data; Main, P.; Fiske, S. J.; Hall, S. E.; Lessinger, L.; Germain, G.; Declerq, J.-P.; Woolfson, M. M. Universities of York and Louvian, 1982.

(47) Allen, F. H.; Kennard, O.; Watson, D. G.; Brammer, L.; Orpen, A. G.; Taylor, R. *J. Chem. Soc., Perkin Trans. II* **1987**, S1. Neutron data: (C–H, 1.083 Å; N–H, 1.009 Å; O–H, 0.983 Å).